Growth of the coccolithophore *Emiliania huxleyi* in light- and nutrient-limited batch reactors: relevance for the BIOSOPE deep ecological niche of coccolithophores

Laura Perrin[1], Ian Probert[2], Gerald Langer[3] and Giovanni Aloisi[4]

[1]Sorbonne Universités, UPMC Univ. Paris 06 -CNRS-IRD-MNHN, LOCEAN-IPSL, 75252 Paris, France.

[2]CNRS-UPMC Univ. Paris 06 FR2424, Roscoff Culture Collection, Station Biologique de Roscoff, 29680 Roscoff, France.

[3]The Marine Biological Association of the United Kingdom, The Laboratory, Citadel Hill, Plymouth, Devon, PL1 2PB, UK.

[4]LOCEAN, UMR 7159, CNRS-UPMC-IRD-MNHN, 75252 Paris, France.

Correspondence to: L. Perrin (lpelod@locean-ipsl.upmc.fr)

Abstract. Coccolithophores are unicellular calcifying marine algae that play an important role in the oceanic carbon cycle via their cellular processes of photosynthesis (a CO_2 sink) and calcification (a CO_2 source). In contrast to the well-studied, surface-water coccolithophore blooms visible from satellites, the lower photic zone is a poorly known but potentially important ecological niche for coccolithophores in terms of primary production and carbon export to the deep ocean. In this study, the physiological responses of an *Emiliania huxleyi* strain to conditions simulating the deep niche in the oligotrophic gyres along the BIOSOPE transect in the South Pacific gyre were investigated. We carried out batch culture experiments with an *E. huxleyi* strain isolated from the BIOSOPE transect, reproducing the in situ conditions of light- and nutrient- (nitrate and phosphate) limitation. By simulating coccolithophore growth using an internal stores (Droop) model, we were able to constrain fundamental physiological parameters for this *E. huxleyi* strain. We show that simple batch experiments, in conjunction with physiological modelling, can provide reliable estimates of fundamental physiological parameters for *E. huxleyi* that are usually obtained experimentally in more time-consuming and costly chemostat experiments. The combination of culture experiments, physiological modelling and in situ data from the BIOSOPE cruise shows that *E. huxleyi* growth in the deep BIOSOPE niche is co-limited by availability of light and nitrate. This study contributes more widely to the understanding of *E. huxleyi* physiology and behavior in a low-light and oligotrophic environment of the ocean.

Keywords

Coccolithophores, batch cultures, deep niche, South Pacific Gyre, Droop model, physiological parameters.

1. Introduction

Coccolithophores are unicellular photosynthetic and calcifying algae that are very abundant in the marine environment and play key roles in the global carbon cycle (Paasche, 2002; Roth, 1994). Through photosynthesis they contribute to the upper ocean carbon pump (CO_2 sink), while via calcification they contribute to the carbonate counter-pump (CO_2 source) (Paasche, 2002; Westbroek et al., 1993). The relative importance of calcification and photosynthesis is one of the factors that dictates the effect of coccolithophores on ocean-atmosphere CO_2 fluxes (Shutler et al., 2013). Environmental conditions such as temperature, irradiance, nutrient concentrations and pCO_2 exert a primary control on the calcification/photosynthesis ratio in coccolithophores and also affect cellular growth rates, which, together with grazing, mortality, sinking of cells and oceanic transport, define the biogeography of coccolithophores. Despite the fact that certain coccolithophores have been fairly extensively studied in the laboratory (e.g. Daniels et al., 2014; Iglesias-Rodriguez et al., 2008; Krug et al., 2011; Langer et al., 2012; Rouco et al., 2013), the factors controlling their biogeography in the global ocean are poorly understood (Boyd et al., 2010). In controlled laboratory conditions, coccolithophore growth is monitored as given environmental parameters are varied (e.g. Buitenhuis et al., 2008; Feng et al., 2008; Fritz, 1999; Langer et al., 2006; Leonardos and Geider, 2005; Paasche, 1999; Trimborn et al., 2007). In the ocean, geographical surveys of coccolithophore abundance and concomitant measurements of environmental variables contribute to defining coccolithophore biogeography in relation to the environment (Claustre et al., 2008; Henderiks et al., 2012). Although extrapolation of results from laboratory experiments to field distributions might not be straightforward, this approach has been widely used and continues to yield important insights into coccolithophore ecology and theirs reactions to a rapidly changing environment.

In this respect, one of the least well understood, but possibly globally relevant niches where coccolithophores can be relatively abundant is that occurring at the deep pycnocline of oceanic gyres, probably the best studied example of which was observed during the BIOSOPE cruise in the South Pacific Gyre (Beaufort et al., 2008; Claustre et al., 2008). This deep coccolithophore niche occurred at about 200 m depth, at a very low irradiance level (< 20 µmol photons m^{-2} s^{-1}) and at a depth corresponding to the nitrate and phosphate nutricline with dissolved nitrate (NO_3) and phosphate (PO_4) concentrations of about 1 µM and 0.2 µM, respectively. The niche was dominated by coccolithophore species belonging to the family Noëlaerhabdaceae, i.e. *Emiliania huxleyi* and species of G*ephyrocapsa* and *Reticulofenestra* (Beaufort et al., 2008). Deep-dwelling coccolithophores have also been observed in other geographic regions. Okada and McIntyre (1979) observed coccolithophores in the North Atlantic Ocean down to a depth of 100 m where *Florisphaera profunda* dominated assemblages in summer and *E. huxleyi* for the rest of the year. Deep coccolithophore populations dominated by *F. profunda* in the lower photic zone (LPZ > 100 m) of subtropical gyres were observed by Cortés et al. (2001) in the Central North Pacific Gyre (station ALOHA)

and by Haidar and Thierstein (2001) in the Sargasso Sea (North Atlantic Ocean). Jordan and Winter (2000) reported assemblages of coccolithophores dominated by *F. profunda* in the LPZ in the north-east Caribbean with a high abundance and co-dominance of *E. huxleyi* and *G. oceanica* through the water column down to the top of the LPZ. These deep-dwelling coccolithophores are not recorded by satellite-based remote sensing methods (Henderiks et al., 2012; Winter et al., 2014) that detect back-scattered light from coccoliths from a layer only a few tens of meters thick at the surface of the ocean (Holligan et al., 1993; Loisel et al., 2006).

Understanding the development of deep coccolithophore populations in low nutrient, low irradiance environments would contribute to building a global picture of coccolithophore ecology and biogeography. Laboratory culture experiments with coccolithophores that combine both nutrient and light limitation, however, are scarce. One reason is that investigating phytoplankton growth under nutrient limitation in laboratory experiments is complicated. In batch cultures the instantaneous growth rate decreases as nutrients become limiting, making it hard to extract the dependence of growth rate on nutrient concentrations (Langer et al., 2013). This can be avoided by employing chemostat cultures, in which growth rates and nutrient concentrations are kept constant under nutrient-limited conditions (Engel et al., 2014; Leonardos and Geider, 2005; Müller et al., 2012). Physiological parameters obtained in chemostat experiments have been used in biogeochemical models to investigate environmental controls on phytoplankton biogeography (Follows and Dutkiewicz, 2011; Gregg and Casey, 2007). Despite their relevance to nutrient limited growth, chemostat cultures are relatively rarely used because they are more expensive, time-consuming and complicated to set up and run than batch cultures (LaRoche et al., 2010).

In this study, we investigated growth of the coccolithophore *E. huxleyi* under light and nutrient co-limitation and applied the results of this culture study to investigate the conditions controlling growth in the deep niche of the South Pacific Gyre. Using an *E. huxleyi* strain isolated during the BIOSOPE cruise, we carried out batch culture experiments that reproduced the low in situ light and nutrient conditions of the deep ecological niche. We monitored the nitrogen and phosphorus content of particulate organic matter, as well as cell, coccosphere and coccolith sizes, because these parameters are known to vary with nutrient limitation (Fritz, 1999; Kaffes, 2010; Rouco et al., 2013). To overcome the conceptual limitations inherent in nutrient-limited batch experiments (Langer et al., 2013), we modeled the transient growth conditions in the batch reactor assuming that assimilation of nutrients and growth are either coupled (Monod, 1949) or decoupled (Droop, 1968) processes in the coccolithophore *E. huxleyi*. An independent check of our modelling approach was obtained by also modeling the *E. huxleyi* batch culture data of Langer et al. (2013). The range of physiological parameters that can be directly assessed in batch culture experiments is limited (Eppley et al., 1969; Marañón et al., 2013). We show that batch cultures, if coupled to simple physiological modeling, may provide valuable estimates of fundamental physiological parameters that are more widely

obtained in more time-consuming and costly chemostat experiments (Eppley and Renger, 1974; Terry, 1982; Riegman et al., 2000; Müller et al., 2012). Our joint culture and modelling approach also provides information on the conditions that control the growth of *E. huxleyi* in the deep ecological niche of the South Pacific Gyre.

2. Materials and methods

2.1 Experimental

2.1.1 Growth medium and culture conditions

Natural seawater collected near the Roscoff Biological Station (Brittany, France) was sterile-filtered and enhanced to K (-Si,-Tris, +Ni, -Cu) medium according to Keller et al. (1987), with only nitrate (no ammonium) as a nitrogen source. *Emiliania huxleyi* strain RCC911, isolated in summer 2004 from a water sample collected at 10 m depth near the Marquesas Islands during the BIOSOPE cruise (November to December 2004), was grown in batch cultures. Experiments were conducted in triplicate in 2.7 litre polycarbonate bottles (Nalgene) with no head space. Experimental conditions were chosen to reproduce those prevalent in surface waters and at the nitricline of the oligotrophic gyre in the South Pacific Ocean (Morel et al., 2007). Cultures were grown under a 12:12 hour light:dark (L:D) cycle (taken from a calculation of L:D cycle at the GYR station at the date of the sampling), at a temperature of 20°C and at a salinity of 34.7. Cultures were grown at two irradiance levels: high light (ca. 140 µmol photons m^{-2} s^{-1}) and low light (ca. 30 µmol photons m^{-2} s^{-1}). The latter corresponds to the upper end of the irradiance range of the deep BIOSOPE coccolithophore niche (10-30 µmol photons m^{-2} s^{-1}). We chose not to run experiments at irradiance levels lower than 30 µmol photons m^{-2} s^{-1} in order to avoid very long experimental runs. Nutrient concentrations at the beginning of batch experiments were 100 µM and 2.5-5.1 µM for nitrate and 6.25 and 0.45-0.55 µM for phosphate in nutrient-replete and nutrient-limited conditions, respectively. For each irradiance level, three experiments were carried out (in triplicate): control (nutrient-replete), phosphate limited (P-limited) and nitrate limited (N-limited) conditions. Cells were acclimated to light, temperature and nutrient conditions for at least three growth cycles prior to experiments.

2.1.2 Cell enumeration and growth rate

The growth of batch cultures was followed by conducting cell counts every day or every other day using a BDFacs Canto II flow cytometer. Experiments were stopped before the cell density reached ca. $1.5*10^5$ cells mL^{-1} in order to minimize shifts in the dissolved inorganic carbon (DIC) system. Cultures remained in the exponential growth phase throughout the duration of the control (nutrient-replete) experiments. In these control cultures, the growth rate (µ) was obtained by conducting a linear regression of the cell density data on the logarithmic scale. Nutrient-limited experiments were allowed to run until growth stopped. The growth rate in nutrient limited conditions decreases in time as nutrients are depleted and it is therefore not possible to calculate growth rate by means of regression analysis (Langer et al.,

2013). The dependence of growth rate on nutrient concentration in nutrient-limited conditions was investigated with the numerical model introduced in Sect. 2.2 below.

2.1.3 Cell and coccosphere diameter and coccolith length

Samples were taken at the end of the experiments at roughly the same point in the L:D cycle (between noon and 4pm) to acquire images of cells using an optical microscope (x100, oil immersion, Olympus BX51 microscope). The internal cell diameter of 100 cells was measured for each experimental culture using the ImageJ software (http://rsbweb.nih.gov/ij/). Images of coccospheres and coccoliths were obtained with scanning electron microscopy (SEM). For SEM observations, samples were filtered onto 0.8 µm polycarbonate filters (Millipore), rinsed with a basic solution (180 µL of 25 % ammomia solution in 1 litre of MilliQ water) and dried at 55°C for 1 h. After mounting on an aluminum stub, they were coated with gold-palladium and images were taken with a Phenom G2 pro desktop scanning electron microscope. For each experimental culture 100 coccospheres were measured using ImageJ. Three hundred coccoliths per sample were measured using a script (Young et al., 2014) that is compatible with ImageJ in order to measure the distal shield length (DSL) of coccoliths.

2.1.4 Dissolved inorganic carbon (DIC) and nutrient analyses

Subsamples for pH_T (pH on the total scale), DIC and nutrient analyses were taken from culture media at the beginning and at the end of each experiment. The pH was measured with a pHmeter-potentiometer pHenomenal pH1000L with a Ross ultra combination pH electrode on the total scale (precision ± 0.02 pH units) and was calibrated with a TRIS buffer. Samples for the determination of DIC were filtered through pre-combusted (4 h at 450°C) glass-fibre filters (Whatman GF/F) into acid-washed glass bottles and poisoned with mercuric chloride. Bottles were stored at 4°C prior to analysis. A LICOR7000 CO_2/H_2O gas analyzer was used for DIC analysis (precision ± 2 µmol kg^{-1}). A culture aliquot (100 mL) was filtered onto pre-combusted (4 h at 450°C) glass-fibre filters (Whatman GF/F) and stored at -20°C in a polyethylene flask until nutrient analysis. Nitrate and phosphate concentrations were measured using an auto analyzer Seal Analytical AA3 (detection limits were 0.003 µM for PO_4 and 0.01 µM for NO_3).

2.1.5 POC, PON, PIC, POP

For particulate organic carbon (POC), particulate organic nitrogen (PON), and particulate organic phosphorus (POP) analyses, samples (200 or 250 mL) were filtered onto pre-combusted (4 h at 450°C) glass-fibre filters (Whatman GF/F) and preserved at -20°C. POC and PON were measured on the same filter that was dried overnight at 50°C after being placed in a fuming hydrochloric acid dessicator for 2 h to remove coccolith calcite. POC and PON were analyzed using a NC Analyzer Flash EA 1112. Particulate inorganic carbon (PIC) was obtained by using a 7500cx Agilent ICP-MS to analyze the calcium concentration in samples filtered onto 0.8 µm polycarbonate filters (Millipore) and extracted by a 0.4 M solution of nitric acid. PIC was obtained considering a 1:1 stoichiometry between Ca^{2+} and PIC, i.e. all of the calcium on the filters was considered to have come from calcium carbonate (Fagerbakke et al., 1994). POP was determined

as the difference between the total particulate phosphorus and particulate inorganic phosphorus, analyzed using a auto-analyser Seal Analytical AA3, after the filters were placed in a solution of hydrochloric acid, according to the method of Labry et al. (2013).

2.2 Modelling

2.2.1 Monod and Droop model

Growth of *E. huxleyi* in the batch reactors was simulated using Monod and Droop models of cellular growth.

In the Monod model (Monod, 1949), the growth rate depends on the external nutrient concentration and is calculated as:

$$\mu = \mu_{\max} \cdot \frac{[R]}{[R] + K_R} \quad (1)$$

where μ_{max} (in days^{-1}) is the maximum growth rate in nutrient-replete conditions, K_R (in µmol L^{-1}) is the (Monod) half-saturation constant for growth and *[R]* (in µmol L^{-1}) is the concentration of nutrient R in the batch reactor. Both μ_{max} and K_R were obtained by fitting the model to the data, while *[R]* is the nutrient concentration in the culture experiments calculated as detailed below.

Two differential equations keep track of the total cell abundance in the batch reactor (*Cells*) and the limiting nutrient concentration in the reactor:

$$\frac{dCells}{dt} = \mu \cdot Cells \quad (2)$$

$$\frac{d[R]}{dt} = \frac{-R_{UP} \cdot Cells}{V} \quad (3)$$

where *V* (in litres) is the volume of the batch reactor, *Cells* (in cells mL^{-1}) is the cell density measured during the experiments, and R_{UP} the cell-specific R uptake rate (in µmol$_R$ cell^{-1} d^{-1}) given by:

$$R_{UP} = \mu \cdot Q_R \quad (4)$$

where Q_R, the (constant) cellular quota of nutrient R (in µmol$_R$ cell^{-1}) is the value of the quota R at the end of the control experiment.

In the Droop model (Droop, 1968) nutrient uptake and cellular growth are decoupled and cellular growth depends on the internal store of the limiting nutrient. The time-dependent rate of nutrient uptake, R_{up} (in µmol$_R$ cell^{-1} d^{-1}), is simulated using Michaelis-Menten uptake kinetics:

$$R_{up} = S_{cell} \cdot V_{\max R} \cdot \frac{[R]}{[R] + K_R} \quad (5)$$

where S_{Cell} (in μm^3) is the surface area of the cell, V_{maxR} (in $\mu mol_R\ \mu m^{-2}\ d^{-1}$) is the maximum surface-normalized nutrient uptake rate (obtained by fitting the model to the data) and K_R (in $\mu mol\ L^{-1}$) is the (Michaelis-Menten) half-saturation constant for uptake of nutrient R. The volume and surface of cells (S_{cell}) was obtained either by measurements of cells (both in the control culture and at the end of the nutrient-limited cultures) for the RCC911 strain experiments, or was estimated from Q_C, the cellular organic carbon quota (in $pmol_C\ cell^{-1}$), and the density of carbon in coccolithophore biomass (approximately equal to 0.015 $pmol_C\ \mu m^{-3}$; Aloisi, 2015) for the batch experiments of Langer et al. (2013) for which cell measurements were not made.

The phytoplankton growth rate μ (in d^{-1}) was calculated based on the normalized ^{n}Quota equation reported in Flynn (2008):

$$\mu = \mu_{\max} \cdot \frac{(1 + KQ_R) \cdot (Q - Q_R^{\min})}{(Q - Q_R^{\min}) + KQ_R \cdot (Q_R^{\max} - Q_R^{\min})} \quad (6)$$

where μ_{max} (in d^{-1}) is the maximum growth rate attained at the maximum nutrient cell quota Q_R^{max} (in μmol $cell^{-1}$), Q_R^{min} (in μmol $cell^{-1}$) is the minimum (subsistence) cellular quota of nutrient R below which growth stops and KQ_R is a dimensionless parameter that can be readily compared between nutrient types and typically has different values for NO_3 and PO_4 (Flynn, 2008). While Q_R^{max} was obtained from the analysis of the nutrient quota (N or P) at the end of the control experiments, Q_R^{min} was estimated by calculation described in the Sect. 2.2.2 below and KQ_R was obtained from fitting the model to the experimental data. Thus, in the Droop model, the growth rate depends on the internal cellular quota of nutrient R, rather than on the external nutrient concentration like in the Monod model of phytoplankton growth.

Three differential equations keep track of the total cell abundance in the batch reactor (*Cells*), the nutrient concentration in the reactor (*[R]*, in μmol L^{-1}) and the internal cellular quota of nutrient (Q_R, in μmol $cell^{-1}$):

$$\frac{dCells}{dt} = \mu \cdot Cells \quad (7)$$

$$\frac{d[R]}{dt} = \frac{-N_{up} \cdot Cells}{V} \quad (8)$$

$$\frac{dQ_R}{dt} = N_{up} - \mu \cdot Q_R \quad (9)$$

These three differential equations are integrated forward in time starting from initial conditions chosen based on experimental values of the number of cells, nutrient concentration at the beginning of the experiment and the cellular nutrient quota determined during growth in nutrient-replete conditions.

The dependence of the maximum growth rate on irradiance was determined independently by fitting the growth rate determined in the exponential growth phase in our experiments and in the experiment of Langer et al. (2013) to the following equation from MacIntyre et al. (2002):

$$\mu = \mu_{\max}\left(1 - e\left(\frac{-Irr}{K_{Irr}}\right)\right) \quad (10)$$

where K_{Irr} is the light-saturation parameter of growth in µmol photons m^{-2} s^{-1} (MacIntyre et al., 2002; Fig. S1) and was determined by this equation.

2.2.2 Modelling strategy

The Droop model presented here does not take into account the variation of size of coccolithophore cells between the different experiments. This model has eight parameters. Four are considered to be known and constant for a given experiment: batch volume *V*, cell volume (and surface area S_{Cell}), and minimum and maximum cellular quota of nutrient, respectively Q_{min} and Q_{max}. The unknown parameters (the physiological parameters of interest) are: the (Michaelis-Menten) half-saturation constant for nutrient uptake K_R, the maximum surface-normalized nutrient uptake rate V_{maxR}, the maximum growth rate μ_{max} and the dimensionless parameter KQ_R. The Monod model has fewer known parameters: batch volume *V* and cellular quota of nutrient $Q_{R.}$ Unknown parameters are: maximum growth rate μ_{max} and the (Monod) half-saturation constant for growth K_R.

Concerning Q_R^{min}, the measured minimum PON value (5.71 fmol $cell^{-1}$) for the N-limited experiment of Langer et al. (2013) is very low compared with the PON quota in other N-limited *E. huxleyi* experiments reported in the literature (38.9-39.3 fmol $cell^{-1}$ in Sciandra et al., 2003; and 51.4 fmol $cell^{-1}$ in Rouco et al., 2013). When the Q_N^{min} value of Langer et al. (2013) was used in the model, the model fit to the experimental data degraded considerably (data not shown). Consequently, we decided to recalculate Q_N^{min} using the initial concentration of dissolved N and the final cell density in the reactor (column "Calculation" in Table 3). This calculated value of Q_N^{min}, that in all cases except for the N-limited experiments of Langer et al. (2013) was very similar to the measured minimum PON quota, was comparable to values reported in the literature for *E. huxleyi* and resulted in a very good fit of the model to the experimental data. To be coherent, we applied this approach to all values of Q_N^{min} and Q_P^{min} used in the modelling exercise.

A point to note concerning the Q_P^{max} used for the P-limited experiment of Langer et al. (2013) is that the initial C:P ratio for the control experiment was 214, which is much higher than the Redfield ratio of 106

(Redfield, 1963). It is not possible to reproduce the experimental data when imposing such a high C:P ratio in the model. Thus, the Q_P^{max} value had to be increased in order to reproduce the data and thus estimate additional physiological parameters for this experiment. For this reason, the modelling results for this particular experiment should be taken with caution.

The time-dependent cell density, limiting nutrient concentration and cellular particulate organic nitrogen and phosphorus calculated by the models were fitted to the same quantities measured in the experiments. For our experiments there were only two nutrient cellular quota data points, one at the beginning and one at the end of the experiments. We artificially inserted a third nutrient-quota data point at the end of the exponential growth phase, setting it equal to the nutrient quota at the beginning of the experiment. In this way the model is forced to keep the nutrient quota unchanged during the exponential growth phase. This is a reasonable assumption, as cellular nutrient quotas should start to be affected only when nutrient conditions become limiting.

The quality of the model fit to the experimental data was evaluated with a cost function. For a given model run, the total cost function was calculated as follows:

$$TotCost = \sum_{i=1}^{n} (\Delta x_i)^2 \quad (11)$$

where n is the number of data points available and ΔX_i is the difference between the data and the model for the i^{th} data point:

$$\Delta x_i = Data(x_i) - Model(x_i) \quad (12)$$

where X_i is the data or model value for the considered variable (cell density, limiting nutrient concentration or cellular limiting nutrient quota). The lower the cost function is, the better the quality of the model fit to the data. For a given experiment, the best-fit of the model to the data was obtained by running the model repeatedly imposing a high number of combinations of input parameters (typically 500000 model runs for every experiment) and selecting the parameter setting that yielded the lowest cost.

3. Results

3.1 Laboratory experiments with E. huxleyi strain RCC911

Growth curves for all experiments with *E. huxleyi* strain RCC911 are shown in Fig. 1. Experiments run in high light conditions attained target cell densities (in nutrient-replete, control experiments) or nutrient limitation (in nutrient-limited experiments) in a shorter time compared to experiments run in low light conditions. Growth in nutrient-replete cultures in both light conditions followed an exponential growth

curve (growth rates in the control nutrient-replete experiments were 0.91 ± 0.03 d^{-1} and 0.28 ± 0.01 d^{-1} for the high light and low light experiments, respectively; Table 1) whereas in nutrient-limited experiments growth evolved from an exponential to a stationary phase at the end of the experiment, except the P-limited culture at low light where the stationary phase was not attained (growth rate of 0.13 ± 0.01 d^{-1}).

In the high light experiment, NO_3 concentration decreased to 0.18 ± 0.03 µM in N-limited cultures and PO_4 concentration decreased to 0.011 ± 0.004 µM in P-limited cultures at the end of the experiments, and in low light conditions the final NO_3 and PO_4 concentrations were 0.13 ± 0.02 µM and 0.008 ± 0.006 µM, respectively (Table 1). Thus, nutrients where nearly completely exhausted at the end of our nutrient-limited experiments. Seawater carbonate chemistry was quasi-constant over the course of the experiments in all treatments, with, as reported by Langer et al. (2013), the P-limited cultures undergoing the largest change in DIC (12-13%; Table 1).

Compared to the control experiments, cellular POC, PIC and PON quotas increased in the P-limited cultures at both light levels, while cellular POP quota decreased (Table 2; Fig. 2D). In the N-limited cultures, cellular PIC and POC quotas (Fig. 2A and B) increased, with the exception of POC at low light that remained nearly unchanged, while cellular PON and POP quotas (Fig. 2C and D) decreased at both light levels. N-limiting conditions resulted in an increase of the POC:PON ratio in both light regimes (Fig. 3A, Table 2). POC:POP (Fig. 3B) was higher in P-limited experiments compared to nutrient-replete experiments. The PIC:POC ratio increased with both N- and P-limitation (Fig. 3C) at both light regimes. For the high light experiment, the PIC:POC ratio was highest in the P-limited culture (0.52 ± 0.14), while in the low light conditions, the highest ratio was recorded in the N-limited culture (0.33 ± 0.02) (Fig. 3C).

Light limitation led almost invariably to a decrease in POC and PIC, with the exception of POC in nutrient-replete conditions (Table 2, Fig. 2). In P-limited cultures POP and PON decreased with light limitation, whereas in N-limited cultures POP and PON increased with light limitation (Fig. 2). With the exception of the POC:POP ratio in P-limiting conditions that was not affected by the change in light regime, both POC:PON and POC:POP ratios decreased with light limitation. Finally, the PIC:POC ratio decreased with light limitation in all three nutrient conditions.

Cell size varied with both nutrient and light limitation (Table S1). Compared to the control culture, in high light conditions, the cell volume was higher for the P-limited culture (77.2 ± 19.9 μm^3) and was similar for the N-limited culture (47.33 ± 11.13 μm^3). The same pattern was observed in low light conditions. P-limitation resulted in higher coccosphere volume and higher DSL than the other nutrient conditions in both light regimes (Table S1). For example, the coccosphere volume in high light was 260 ± 88 μm^3 for the P-limited experiment, whereas it was 109 ± 23 μm^3 for the control experiment and 139 ± 41 μm^3 for the N-limited experiment. There was no measurement of coccosphere volume and DSL in the low light control culture because of a lack of visible cells on the filters. However, the coccosphere volume for the P-limited

treatment followed the same trend as the cell size, i.e. a decrease with lower light. Figure 4A shows the correlation between POC content and cell volume (R^2=0.85, p<0.05, n=6) and figure 4B between cell and coccosphere volume (R^2=0.92, p<0.03, n=5). Relationships between DSL and coccosphere size (R^2=0.68, p<0.3, n=5) and between DSL and cell size (R^2=0.86, p<0.06, n=5) are illustrated in figure 4C. These parameters were not significantly correlated, but the sample size was rather low. The thickness of the coccolith layer, calculated by subtracting the cell diameter from the coccosphere diameter and dividing by two, was higher for P-limited cultures in both light conditions: 1.294 ± 0.099 µm for high light and 1.02 ± 0.043 µm for low light compared with the other cultures which were between 0.66 and 1 µm. These observations are consistent with the high PIC quota and relatively large size of coccospheres and coccoliths of *E. huxleyi* under P-limitation.

3.2 Modelling results

We applied the modelling approach to both the data from our batch culture experiments with strain RCC911 and to the batch culture data of Langer et al. (2013) who tested N- and P-limited growth of *E. huxleyi* strain PML B92/11 cultured in high light conditions (400 µmol photons m^{-2} s^{-1}), optimal temperature (15°C) and quasi-constant carbon system conditions. Measurements of cell density, nutrient concentrations and cellular particulate matter from both sets of experiments were used for the present modelling study.

The Droop model was able to accurately reproduce both experimental data sets (Fig. 5, 6 and 9; Fig. S2, S3 and S4), whereas the Monod model was not able to reproduce the rise in cell number after the limiting nutrient had been exhausted (Fig. 5). The modelling approach allows evaluation of the evolution of experimental variables that are complicated to determine analytically, i.e. (1) the nutrient-uptake rate, that follows the same trend as the nutrient concentration in the reactor, (2) the C/limited-nutrient ratio, that starts at a minimum value, stays constant during the duration of the exponential phase and then increases due to exhaustion of the external nutrient, reaching a maximum as the culture attains the stationary phase, and (3) the instantaneous growth rate, that follows the trend of the limiting nutrient ratio, reaching zero when the culture attains the stationary phase.

The values for the physiological parameters of the best-fit obtained by applying the Droop model to our experiments with *E. huxleyi* strain RCC911 and to the experiments of Langer et al. (2013) are presented in Table 3. Overall, the best-fit values for the two strains in high light conditions were very similar, suggesting that the modelling approach is sound. Values for the half-saturation constant for nitrate uptake K_N determined in our experiments in high light conditions and in those of Langer et al. (2013) were comparable. However, for K_P, the value was consistent between our high and low light experiments, but considerably lower for the Langer et al. (2013) experiment, which, as noted above, is a result that should be taken with caution. The maximum surface nutrient-uptake rate V_{max} were similar between our high light experiment and that of Langer et al. (2013). The dimensionless parameters KQ_N and KQ_P were also

374 comparable between the two studies for high light conditions and in both cases KQ_P was higher than KQ_N.
375 Maximum growth rates in high light conditions were similar for both N-limited and P-limited experiments.
376 As expected, maximum growth rates for our low light cultures were considerably lower (Table 3).
377 To test the reliability of the model to obtain estimates of the physiological parameters, we forced the
378 model to run with a range of values for a given parameter, while letting the other three parameters vary
379 over a wide range. These tests give us plots of the value of the cost function (Eq. 9) as a function of the
380 value of the imposed parameter. The process was repeated separately for the four unknown parameters
381 and Fig. S5 shows the results for the N-limited culture of Langer et al. (2013). For all of the parameters
382 except for K_R, this exercise yielded a U-shaped curve with a minimum of the cost function corresponding to
383 the best-fit parameter values presented in Table 3. This shows that the model is well suited to find a best-fit
384 value for these parameters. Three minima of the cost function were found for K_R (Fig. S5) of which only the
385 lowest was consistent with values reported in the literature (e.g. Riegman et al., 2000). This value was
386 chosen to obtain the best-fit of the model to the experimental data.
387

388 ## 4. Discussion

389 ### *4.1 Batch culture experiments*

390 The batch culture experiments presented here provide new insights into the physiology of the
391 numerically dominant coccolithophore *E. huxleyi* under conditions of light and nutrient limitation.
392 Leonardos and Geider (2005) carried out cultures in low light and low phosphate conditions with a non-
393 calcifying *E. huxleyi* strain and thus did not report PIC:POC ratios. The culture study reported here is thus
394 the first experiment where changes in the PIC:POC ratio due to light-limitation are explored for nutrient-
395 limited cultures. In our experiments, cultures were harvested at relatively low cell densities, i.e. a maximum
396 of ca. $1.6*10^5$ cells mL^{-1} in the P-limited low light experiment and < $1.3*10^5$ cells mL^{-1} in all other
397 treatments. The aim was to ensure that changes in the carbonate system were within a minimal range (<
398 10% except for the P-limited experiments in which the DIC changes were 12 and 13%; Table 1) that is not
399 expected to have a significant influence on measured physiological parameters (Langer et al., 2007;
400 LaRoche et al., 2010). Hence, it can be stated that the observed phenomena stem from N-/P-limitation
401 and/or light limitation (depending on the treatment) rather than from carbon limitation.
402 Comparison of the growth curves illustrated in Fig. 1 demonstrates that growth limitation was attained
403 in both our low nutrient and low light treatments relative to control conditions. Consistent with previous
404 experimental results (Langer et al., 2013; Leonardos and Geider, 2005; Müller et al., 2012; Oviedo et al.,
405 2014; Rouco et al., 2013), the relatively low cellular PON or POP quotas (and high POC:PON and POC:POP
406 ratios) at the end of the low nutrient experiments relative to the control indicate that nutrient limitation of
407 growth occurred in our low nutrient experiments. The stationary phase was not attained in the P-limited
408 low light culture, but it can be inferred that cells were P-limited from: (a) the POP quota, which was lower

than that of the control, (b) the POC:POP ratio, which was higher than that of the control, and (c) a deviation of the growth curve from exponential growth starting (at the latest) on day 16 of 19. While a decline in POP quota is an early sign of limitation, the decline in growth rate occurs later, indicating more severe limitation. The cessation of cell division (stationary phase) would be the last stage in the process of becoming fully P-limited over the course of a batch culture.

In nutrient-replete conditions, low light had no effect on POC quota (Fig. 2) and cell size (Fig. 4) within the limit of uncertainty of the measurements, whereas it caused a decrease in PIC quota (and therefore a decrease in PIC:POC ratio). Although PIC quota also decreased in low light for nutrient-limited conditions (Fig. 2), the PIC quota for nutrient-replete conditions in low light was unexpectedly low indicating a potential anomaly in the calcification process for this experiment.

In our experiments N-limitation led to an increase in the PIC:POC ratio in both high and low light conditions, a result that is consistent with most previous N-limitation studies with *E. huxleyi* (see review by Raven and Crawfurd, 2012), but the cause of this increase appears to vary. According to Müller et al. (2008) and Raven and Crawfurd (2012), N-limited cells decrease in volume due to substrate limitation and lower assimilation of nitrogen in the G1 phase of the cell division cycle, but in our experiments N-limitation did not cause an obvious decrease in cell volume or POC quota, but rather an increase in PIC quota relative to nutrient-replete cells in both high and low light conditions (Fig. 2) (Table S1). Both Müller et al. (2008) and Fritz (1999) also reported an increase of the PIC content of *E. huxleyi* in N-limited conditions. The increase in PIC quota is difficult to explain in light of the observations that coccolith size was lower in N-limited cultures and coccosphere volume was broadly comparable (given the error margins) in control and N-limited cultures (Fig. 4).

P-limitation had the greatest effect on cell size, cells being significantly larger under P-limitation than in control conditions, for both high and low light regimes. The increase in cell volume was accompanied by increases in both POC and PIC quotas, again in both light conditions (Fig. 2). According to Müller et al. (2008), P-limitation inhibits DNA replication while biomass continues to build up, leading to an increase in cell volume. This could explain the very high volume of P-limited cells in high light conditions in our experiments, and the slightly increased cell volume in the P-limited, low light experiment, compared to experiments not limited by PO_4. P-limitation resulted in a considerably higher coccosphere volume than the other nutrient conditions, in line with the observations of Müller et al. (2008) and Oviedo et al. (2014). In high light the PIC quota in P-limited cells was more than tripled relative to nutrient-replete conditions. This general effect of phosphate limitation was also reported by Raven and Crawfurd (2012) (Table 2) and is likely due to the occurrence of larger (as shown by high DSL values) and potentially more numerous coccoliths (Gibbs et al., 2013). In the P-limited experiment, PIC:POC ratios increased relative to nutrient-replete cultures, like in the experiments of van Bleijswijk et al. (1994) and Berry et al. (2002), although Oviedo et al. (2014) reported that the response of the PIC:POC ratio to P-limitation is strain-specific in *E.*

huxleyi. The increase in PIC:POC in *E. huxleyi* is often greater for P-limitation than for N-limitation (Zondervan, 2007), as for our high light experiment. However, in low light the PIC:POC ratio was higher under N-limitation, highlighting that co-limitation can have unexpected physiological consequences.

In our experiments the PIC:POC ratio decreased with light limitation in nutrient replete and nutrient limited conditions (Fig. 3). Zondervan (2007) stated that the ratio of calcification to photosynthetic C fixation increases with decreasing light intensities due to the lower saturation irradiance for calcification than photosynthesis in *E. huxleyi*. However, due to a more rapid decline of calcification relative to photosynthesis below saturation levels this ratio decreases again under strongly light-limiting conditions (below approximately 30 µmol photons m^{-2} s^{-1}). Several culture studies using different *E. huxleyi* strains have reported this trend. Using the same L:D cycle (12:12) as employed in our experiments, Feng et al. (2008) also reported a decreasing PIC:POC ratio between 400 and 50 µmol photons m^{-2} s^{-1}. Comparable observations have been reported in studies that used a 16:8 L:D cycle with decreasing light from 300 down to a minimum of 30 µmol photons m^{-2} s^{-1} (Trimborn et al., 2007; Rokitta and Rost, 2012). Again with a 16:8 L:D cycle, Rost et al. (2002) reported a decrease of the PIC:POC ratio between 80 and 150 µmol photons m^{-2} s^{-1} (for a pCO_2 level comparable to that in our experiments), but an increase of the ratio with an increase of the irradiance from 15 to 30 and to 80 µmol.m^{-2}.s^{-1}. Our results indicate that calcification was more severely limited than photosynthesis at 30 µmol photons m^{-2} s^{-1} in strain RCC911.

The non-significant correlation between DSL and coccosphere size (Fig. 4) is not consistent with the correlation reported by Gibbs et al. (2013) between coccolith and coccosphere size in fossil sediment samples, but the number of observations in our study was too low to draw a robust conclusion about the relationship. The significant correlation between cell and coccosphere volume (Fig. 4) and observations of other studies (e.g. Aloisi, 2015; Gibbs et al., 2013) support the conclusion that coccosphere size in the water column and in sediments could be used as a proxy for cell size (and thus POC quota).

In summary, apart from the phosphate limited low light experiment, nutrient limitation led to a cessation of cell division (entry into stationary phase) at the end of the experiment. Nutrient limitation decreased the particulate organic P or N quota for the limiting nutrient (POP for P-limitation and PON for N-limitation) and increased the PIC:POC ratio under both light conditions. Discerning the effect of nutrient limitation on morphological properties was complicated by the relatively large margins of error, but the overall trend was of an increase in cell/coccosphere size under P-limitation and no obvious effect under N-limitation. Light limitation decreased the PIC quota, tended to decrease the cell size and decreased PIC:POC ratio in every nutrient condition, whereas POC:PON and POC:POP decreased with light limitation. Further investigations need to be carried out to improve the understanding of the effect of light intensity on the PIC:POC ratio.

4.2 E. huxleyi physiological parameters obtained by modelling growth in a batch reactor

In contrast to the Monod model, the Droop model was able to accurately reproduce the experimental data obtained in experiments with *E. huxleyi* strain RCC911 as well as the experiments of Langer et al. (2013). The Droop model was notably able to reproduce the increase in cell number after the limiting nutrient had been exhausted. This indicates that, as for several other phytoplankton groups (Lomas and Glibert, 2000), *E. huxleyi* has the ability to store nutrients internally to continue growth to some extent when external nutrient levels become very low. In our experiments and those of Langer et al. (2013), cells grew on their internal nutrient reserves and managed two to three cell divisions in the absence of external nutrients. These observations are consistent with the explanation of both Monod and Droop models by Bernard (2011).

Numerous studies have estimated the maximum nutrient uptake rate V_{maxR} and the half-saturation constant for nutrient uptake K_R, especially for nitrate uptake, for a variety of phytoplankton species. The values obtained in our study for K_N for high light *E. huxleyi* cultures (Table 3) are comparable to those reported in the literature. Using *E. huxleyi* in chemostat experiments, Riegman et al. (2000) found K_N values between 0.18 and 0.24 µM and K_P between 0.10 and 0.47 µM. In addition, they reported a V_{maxN} of $7.4.10^{-6}$ µmol $cell^{-1}$ d^{-1} which is similar to that found for RCC911 and PML B92/11 (Table 3).

When comparing physiological parameters between phytoplankton taxa, the scaling of physiological parameters with cell size has to be taken into account (Marañón et al., 2013). Marañón et al. (2013) plotted Q_{min} and μ_{max} against cell size (see Fig. 7A for Q_{min} versus cell size) for different phytoplankton species. In these plots coccolithophores fall with the smallest diatoms. Figure 7B reports V_{maxN} versus cell size for different groups of phytoplankton based on the results of Litchman et al. (2007) (using a compiled database) and of Marañón et al. (2013) (22 cultivated species) and the results obtained with the Droop model in this study. Despite the different procedures used to obtain V_{maxN} (simulated with a model or measured experimentally), all values for coccolithophores fall in the same range. Collos et al. (2005) and Litchman et al. (2007) found a linear correlation between the maximum uptake rate and the half-saturation constant for nitrate uptake across several phytoplankton groups (Fig. 7C). This correlation defines a physiological trade-off between the capacity to assimilate nutrients efficiently (high V_{max}) and the capacity to assimilate nutrients in low-nutrient environments (low K_R), and thus thrive in oligotrophic conditions. This analysis shows that large phytoplankton like diatoms and dinoflagellates have high maximum nitrate uptake rates and high half-saturation constant for nitrate uptake. The half-saturation constant for nitrate uptake for *E. huxleyi* is consistently low compared to other groups of phytoplankton, which means that it will be competitive in low nitrate waters (Litchman et al., 2007).

4.3 Controls on E. huxleyi growth in the deep BIOSOPE niche

The BIOSOPE cruise was carried out in 2004 along a transect across the South Pacific Gyre from the Marquesas Islands to the Peru-Chili upwelling zone. The aim of this expedition was to study the biological,

biogeochemical and bio-optical properties (Claustre et al., 2008) of the most oligotrophic zone of the world's ocean (Claustre and Maritorena, 2003). The deep ecological niche of coccolithophores along this transect occurred at the Deep Chlorophyll Maximum (DCM; Beaufort et al., 2008). According to Claustre et al. (2008) and Raimbault et al. (2008), the nitrate concentration at the GYR station at the DCM (between 150 and 200 m depth) was between 0.01 and 1 µM. In our nitrate-limited low light culture experiment (Fig. 8), this concentration occurred between the end of the exponential growth phase and the beginning of the stationary phase (days 8 to 9), when nitrate-limitation began to affect instantaneous growth rates. Claustre et al. (2008) reported a nitrate concentration <3 nM (i.e. below the detection limit) in the 0-100 m water column, whereas phosphate concentration was always above 0.1 µM in surface layers (Raimbault and Garcia, 2008). Moutin et al. (2008) concluded that phosphate was apparently not the limiting nutrient for phytoplankton along the BIOSOPE transect. A potential influence of organic nitrogen sources, that *E. huxleyi* is capable of using (Benner and Passow, 2010), cannot be excluded, but these would be expected to have been distributed vertically in a similar way to NO_3.

The picture that emerges from the figure 9 is consistent with the model of Klausmeier and Litchman (2001), who predicted that growth in a DCM should be limited by both light and one nutrient, with the upper layer of the DCM being limited by nutrient supply and the deeper layer by light. The experiments and modelling work presented here allow us to confirm that growth of *E. huxleyi* in the deep niche at the GYR station of the BIOSOPE transect was clearly limited by light in the lower part of the DCM, and by nitrogen in the upper part of the DCM and upper water column. Nitrification and the vertical diffusivity of nitrate through the nitracline (Holligan et al., 1984) needs to be taken into account and could potentially be a source of dissolved nitrate in the deep niche of coccolithophores. The depth-distribution of the modelled *E. huxleyi* growth rate, and of dissolved nitrogen, light intensity, chlorophyll a concentration and coccolithophore abundance supports the inferred light-nitrate co-limitation (Fig. 9). We used the physiological parameters constrained in our experiments together with a steady state assumption for uptake and assimilation of nitrate (see appendix) to obtain the vertical profile of *E. huxleyi* growth rate at the GYR station (Fig. 9). This calculation, forced by the irradiance and nitrate data from the GYR station, shows that *E. huxleyi* growth rate was maximal at a depth corresponding to that of the measured maximum chlorophyll a concentration. The half-saturation constant for nitrate uptake K_N constrained with the Droop model (0.09 µM) lies within the deep niche (Fig. 9). The maximum estimated growth rate at the GYR station (0.06 d^{-1} at 173 m depth) corresponds to an *E. huxleyi* generation time of 11.5 days, suggesting that division rate at the DCM was extremely slow (0.086 division per day), all the more so since this estimate does not consider grazing and vertical export of cells. Reports of the in situ growth rate of phytoplankton are not common, including for *E. huxleyi*, due to the inherent difficulties in measuring this parameter (Laws, 2013). Goldman et al. (1979) reported phytoplankton doubling times in the North Pacific around 0.36-0.89 per day which corresponds to a growth rate of approximately 0.25 d^{-1}. Selph et al. (2011) estimated growth rates in

552 the equatorial Pacific between 110° and 140°W to be below 0.3 d^{-1} for the phytoplankton community living
553 at 1% of surface irradiance with net growth rates (considering mortality rates) around zero.
554
555 With the above limitation pattern in mind, it is possible to predict the effect of nitrate and light
556 variability on the vertical evolution of the *E. huxleyi* PIC:POC ratio in gyre conditions. According to our
557 experimental results, the PIC:POC ratio increases slightly with nitrate limitation but the strongest effect on
558 PIC:POC ratio seems to be in response to light intensity. As noted above (Section 4.1), several studies have
559 shown that the PIC:POC ratio increases with decreasing irradiance down to 55 ± 25 µmol photons m^{-2} s^{-1},
560 but that it decreases with light limitation below this value. At the BIOSOPE GYR station, the PIC:POC ratio of
561 *E. huxleyi* would be expected to be intermediate in surface waters (nitrate-poor but high light intensity) and
562 then to increase and attain a maximum value in lower subsurface waters down to the upper part of the
563 deep niche (between 80 and 30 µmol photons m^{-2} s^{-1} ; therefore between 110 m and 150 m depth). The
564 PIC:POC ratio would then decrease in the lower part of the deep niche, and finally decrease drastically in
565 deeper, relatively nitrate-rich but extremely low-irradiance waters. This prediction cannot be verified with
566 the available published data from the BIOSOPE transect and PIC:POC ratio of coccolithophores are not only
567 controlled by light and nitrate conditions, but a comparable pattern for the upper part of the ocean was
568 observed through in situ measurements by Fernández et al. (1993). Our predictions need to be verified via
569 in situ studies of DCM zones dominated by coccolithophores. Klaas and Archer (2002) reported that
570 coccolithophores are responsible for the main part of calcium carbonate export to the deep sea and that
571 the rain of organic carbon is mostly associated with calcium carbonate particles, because of their higher
572 density than opal particles and higher abundance than terrigenous material. The gyre ecosystem is a good
573 example of the fact that effects on the rain ratio, and therefore on the carbon pump and carbonate
574 counter-pump, need to be integrated over the whole photic zone. A low PIC quota due to the majority of
575 production occurring at low irradiance in the deep niche would limit the *E. huxleyi*-related calcium
576 carbonate rain to the sediments and potentially also the ballasting of organic carbon to the deep ocean.
577

578 ## 5. Conclusion

579 We present one of the few laboratory culture experiments investigating the growth and PIC:POC ratio
580 of the coccolithophore *E. huxleyi* in light- and nutrient-limited conditions, mimicking those of the deep
581 ecological niche of coccolithophores in the South Pacific Gyre (Beaufort et al., 2008; Claustre et al., 2008).
582 By combining batch culture experiments with a simple numerical model based on the internal stores
583 (Droop) concept, we show that: (1) *E. huxleyi* has the capacity to divide up to several times in the absence
584 of external nutrients by using internal nutrient stores; (2) a simple batch culture experimental set-up
585 combined with a Droop model, as opposed to the more time-consuming and expensive continuous culture
586 approach, can be used to estimate fundamental physiological parameters that describe the response of
587 phytoplankton growth to nutrient availability; (3) the position of the deep coccolithophore niche of the

South Pacific Gyre coincides with the depth of maximum potential growth rate calculated by our physiological model; at shallower depths growth is strongly limited by dissolved nitrate availability, while at greater depths it is strongly limited by the paucity of light. These observations confirm the theoretical prediction of Klausmeier and Litchman (2001) with regard to the environmental controls of growth in the DCM. Our conclusions were based on experiments using *E. huxleyi* strain RCC911 that was isolated from surface waters of the BIOSOPE transect and it will be important to repeat this approach using deep-dwelling strains. There is potential for our approach to shed light on the functioning of other oligotrophic, low-light phytoplankton ecosystems like cold, dark and nutrient-poor Arctic and Antarctic waters.

Appendix

To obtain the growth rate through the vertical profile at the station GYR, we needed to express the cellular quota Q_N as a function of the nitrate concentration NO_3 *[N].* To achieve this, we resolved the system of three equations from the Droop theory:

$$\frac{dQ_N}{dt} = N_{up} - \mu \cdot Q_N \quad \text{(A1)}$$

$$N_{up} = S_{cell} \cdot V_{\max N} \cdot \frac{[N]}{[N] + K_N} \quad \text{(A2)}$$

$$\mu = \mu_{\max} \cdot \frac{(1 + KQ_N) \cdot (Q - Q_N^{\min})}{(Q - Q_N^{\min}) + KQ_N \cdot (Q_N^{\max} - Q_N^{\min})} \quad \text{(A3)}$$

Considering a stationary state (uptake-assimilation steady state) and thus assuming the differential Eq. (A1) equal to zero, we resolved the system to express the cellular quota Q_N versus the nitrate concentration (see Fig. A1):

$$A = \frac{1}{2 \cdot (1 + KQ_N) \cdot \mu_{\max} \cdot (K_N + [N])} \cdot \left((K_N \cdot (1 + KQ_N) \cdot \mu_{\max} \cdot Q_N^{\min}) \right) \quad \text{(A4)}$$

$$B = \left((1 + KQ_N) \cdot \mu_{\max} \cdot [N] \cdot Q_N^{\min} \right) + \left([N] \cdot S_{cell} \cdot V_{\max N} \right) \quad \text{(A5)}$$

$$C = \sqrt{\begin{array}{l} 4(1 + KQ_N) \cdot \mu_{\max} \cdot [N] \cdot (K_N + [N]) \cdot (KQ_N \cdot Q_N^{\max} - (1 + KQ_N) \cdot Q_N^{\min}) \cdot S_{cell} \cdot V_{\max N} \\ + \left((1 + KQ_N) \cdot \mu_{\max} \cdot (K_N + [N]) \cdot Q_N^{\min} + [N] \cdot S_{cell} \cdot V_{\max N} \right)^2 \end{array}} \quad \text{(A6)}$$

$$Q_N = A \cdot (B + C) \quad \text{(A7)}$$

Thus, the growth rate can be expressed depending on the irradiance (and *KIrr*; see Sect. 2.2.1) and the cellular quota Q_N. Physiological parameters are known (output of the model for the experiment in high light and low nitrate conditions):

$$\mu = \mu_{\max} \cdot \frac{(1+KQ_N)\cdot(Q-Q_N^{\min})}{(Q-Q_N^{\min})+KQ_N\cdot(Q_N^{\max}-Q_N^{\min})} \cdot \left(1-e\left(\frac{-Irr}{KIrr}\right)\right) \quad \text{(A8)}$$

The vertical profile of the growth rate of coccolithophores at the GYR station, calculated with this equation, is shown in Fig. 9.

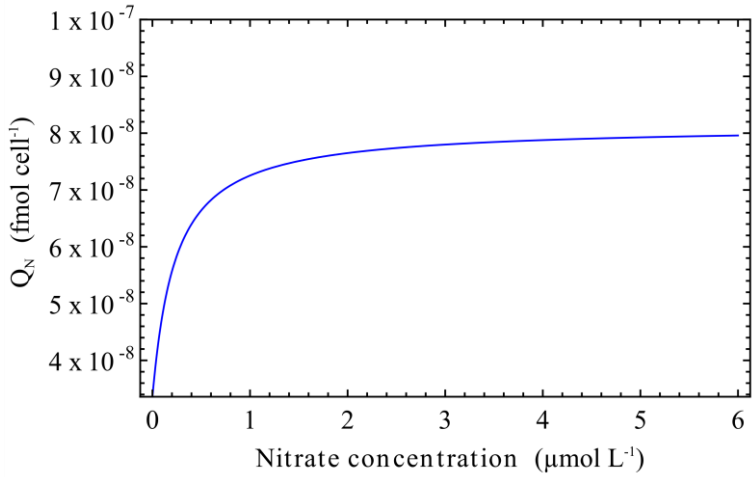

Figure A1. Cellular quota of nitrogen versus the nitrate concentration using parameters of the best-fit results of the model ran for the low light and nitrate limited experiment with RCC911.

Acknowledegements

This project was supported by the TELLUS CLIMAHUX project (INSU-CNRS), the MODIF project of the Institut Pierre Simon Laplace (IPSL), and the CALHIS project (French ANR). We thank C. Schmechtig for providing access to the BIOSOPE database, F. Le Cornec and I. Djouraev for helping with PIC analysis at the Institut de Recherche pour le Développement (IRD) ALYSE platform and C. Labry and A. Youenou for carrying out the POP analysis at IFREMER Centre de Brest. From the Roscoff Biological Station we are grateful to C. Leroux for analysis of POC and PON samples and the Marine Chemistry research team, specifically T. Cariou for dissolved nutrient analyses and acid treatment of POC and PON samples, M. Vernet for help processing DIC samples, and Y. Bozec for DIC analysis. We also thank A. Charantonis for his advice for the modelling methodology. The lead author was supported by a doctoral fellowship from the French Minister of Education and Research (MESR).

References

Aloisi, G.: Covariation of metabolic rates and cell size in coccolithophores, Biogeosciences, 12(15), 6215–6284, doi:10.5194/bg-12-4665-2015, 2015.

Beaufort, L., Couapel, M., Buchet, N., Claustre, H. and Goyet, C.: Calcite production by coccolithophores in the south east Pacific Ocean, Biogeosciences, 5, 1101–1117, 2008.

Benner, I. and Passow, U.: Utilization of organic nutrients by coccolithophores, Mar. Ecol. Prog. Ser. 404, 21–29, 2010.

Bernard, O.: Hurdles and challenges for modelling and control of microalgae for CO2 mitigation and biofuel production, J. Process Control, 21(10), 1378–1389, doi:10.1016/j.jprocont.2011.07.012, 2011.

Berry, L., Taylor, A. R., Lucken, U., Ryan, K. P. and Brownlee, C.: Calcification and inorganic carbon acquisition in coccolithophores, Funct. Plant Biol., 29(3), 289–299, doi:10.1071/PP01218, 2002.

van Bleijswijk, J. D. L., Kempers, R. S., Veldhuis, M. J. and Westbroek, P.: Cell and growth characteristics of types A and B of Emiliania huxleyi (Prymnesiophyceae) as determined by flow cytometry and chemical Analyses, J. Phycol., 30(2), 230–241, doi:10.1111/j.0022-3646.1994.00230.x, 1994.

Boyd, P. W., Strzepek, R., Fu, F. and Hutchins, D. A.: Environmental control of open-ocean phytoplankton groups: Now and in the future, Limnol. Oceanogr., 55(3), 1353–1376, doi:10.4319/lo.2010.55.3.1353, 2010.

Buitenhuis, E. T., Pangere, T., Franklin, D. J., Le Quéré, C. and Malin, G.: Growth rates of six coccolithophorid strains as a function of temperature, Limnol. Oceanogr., 53(3), 1181–1185, doi:10.4319/lo.2008.53.3.1181, 2008.

Claustre, H. and Maritorena, S.: The Many Shades of Ocean Blue, , 302(5650), 1514–1515, 2003.

Claustre, H., Sciandra, A. and Vaulot, D.: Introduction to the special section bio-optical and biogeochemical conditions in the South East Pacific in late 2004: the BIOSOPE program, Biogeosciences, 5(3), 679–691, doi:10.5194/bg-5-679-2008, 2008.

Cortés, M. Y., Bollmann, J. and Thierstein, H. R.: Coccolithophore ecology at the HOT station ALOHA, Hawaii, Deep Sea Res. Part II Top. Stud. Oceanogr., 48(8–9), 1957–1981, doi:10.1016/S0967-0645(00)00165-X, 2001.

Daniels, C. J., Sheward, R. M. and Poulton, A. J.: Biogeochemical implications of comparative growth rates of Emiliania huxleyi and Coccolithus species, Biogeosciences, 11(23), 6915–6925, doi:10.5194/bg-11-6915-2014, 2014.

Droop, M. R.: Vitamin B12 and Marine Ecology. IV. The Kinetics of Uptake, Growth and Inhibition in Monochrysis Lutheri, J. Mar. Biol. Assoc. U. K., 48(3), 689–733, doi:10.1017/S0025315400019238, 1968.

Engel, A., Cisternas Novoa, C., Wurst, M., Endres, S., Tang, T., Schartau, M. and Lee, C.: No detectable effect of CO2 on elemental stoichiometry of Emiliania huxleyi in nutrient-limited, acclimated continuous cultures, Mar. Ecol. Prog. Ser., 507, 15–30, doi:10.3354/meps10824, 2014.

Eppley, R. W. and Renger, E. H.: Nitrogen Assimilation of an Oceanic Diatom in Nitrogen-Limited Continuous Culture, J. Phycol., 10(1), 15–23, doi:10.1111/j.1529-8817.1974.tb02671.x, 1974.

Eppley, R. W., Rogers, J. N. and McCarthy, J. J.: Half-Saturation Constants for Uptake of Nitrate and Ammonium by Marine Phytoplankton, Limnol. Oceanogr., 14(6), 912–920, doi:10.4319/lo.1969.14.6.0912, 1969.

681 Fagerbakke, K. M., Heldal, M., Norland, S., Heimdal, B. R. and Båtvik, H.: Emiliania huxleyi. Chemical
682 composition and size of coccoliths from enclosure experiments and a Norwegian fjord, Sarsia, 79(4), 349–
683 355, doi:10.1080/00364827.1994.10413566, 1994.

684 Feng, Y., Warner, M. E., Zhang, Y., Sun, J., Fu, F.-X., Rose, J. M. and Hutchins, D. A.: Interactive effects of
685 increased pCO2, temperature and irradiance on the marine coccolithophore Emiliania huxleyi
686 (Prymnesiophyceae), Eur. J. Phycol., 43(1), 87–98, doi:10.1080/09670260701664674, 2008.

687 Fernández, E., Boyd, P., Holligan, P. M. and Harbour: Production of organic and inorganic carbon within a
688 large-scale coccolithophore bloom in the northeast Atlantic Ocean, Mar. Ecol. Prog. Ser., 97, 271–285,
689 1993.

690 Flynn, K.: The importance of the form of the quota curve and control of non-limiting nutrient transport in
691 phytoplankton models, J. Plankton Res., 30(4), 423–438, doi:10.1093/plankt/fbn007, 2008.

692 Follows, M. J. and Dutkiewicz, S.: Modeling Diverse Communities of Marine Microbes, Annu. Rev. Mar. Sci.,
693 3(1), 427–451, doi:10.1146/annurev-marine-120709-142848, 2011.

694 Fritz, J. J.: Carbon fixation and coccolith detachment in the coccolithophore Emiliania huxleyi in nitrate-
695 limited cyclostats, Mar. Biol., 133(3), 509–518, doi:10.1007/s002270050491, 1999.

696 Gibbs, S. J., Poulton, A. J., Brown, P. R., Daniels, C. J., Hopkins, J., Young, J. R., Jones, H. L., Thiemann, G. J.,
697 O'Dea, S. A. and Newsam, C.: Species-specific growth response of coccolithophores to Palaeocene–Eocene
698 environmental change, Nat. Geosci., 6, 218–222, doi:10.1038/NGEO1719, 2013.

699 Goldman, J. C., McCarthy, J. J. and Peavey, D. G.: Growth rate influence on the chemical composition of
700 phytoplankton in oceanic waters, Nature, 279(2), 1, 1979.

701 Gregg, W. W. and Casey, N. W.: Modeling coccolithophores in the global oceans, Deep Sea Res. Part II Top.
702 Stud. Oceanogr., 54(5–7), 447–477, doi:10.1016/j.dsr2.2006.12.007, 2007.

703 Haidar, A. T. and Thierstein, H. R.: Coccolithophore dynamics off Bermuda (N. Atlantic), Deep Sea Res. Part
704 II Top. Stud. Oceanogr., 48(8–9), 1925–1956, doi:10.1016/S0967-0645(00)00169-7, 2001.

705 Henderiks, J., Winter, A., Elbrchter, M., Feistel, R., Plas, A. van der, Nausch, G. and Barlow, R.:
706 Environmental controls on Emiliania huxleyi morphotypes in the Benguela coastal upwelling system (SE
707 Atlantic), Mar. Ecol. Prog. Ser., 448, 51–66, doi:10.3354/meps09535, 2012.

708 Holligan, P. M., Balch, W. M. and Yentsch, C. M.: The significance of subsurface chlorophyll, nitrite and
709 ammonium maxima in relation to nitrogen for phytoplankton growth in stratified waters of the Gulf of
710 Maine, J. Mar. Res., 42(4), 1051–1073, doi:10.1357/002224084788520747, 1984.

711 Holligan, P. M., Fernández, E., Aiken, J., Balch, W. M., Boyd, P., Burkill, P. H., Finch, M., Groom, S. B., Malin,
712 G., Muller, K., Purdie, D. A., Robinson, C., Trees, C. C., Turner, S. M. and van der Wal, P.: A biogeochemical
713 study of the coccolithophore, Emiliania huxleyi, in the North Atlantic, Glob. Biogeochem. Cycles, 7(4), 879–
714 900, doi:10.1029/93GB01731, 1993.

715 Iglesias-Rodriguez, M. D., Halloran, P. R., Rickaby, R. E. M., Hall, I. R., Colmenero-Hidalgo, E., Gittins, J. R.,
716 Green, D. R. H., Tyrrell, T., Gibbs, S. J., von Dassow, P., Rehm, E., Armbrust, E. V. and Boessenkool, K. P.:
717 Phytoplankton calcification in a high-CO2 world, Science, 320(5874), 336–340,
718 doi:10.1126/science.1154122, 2008.

719 Jordan, R. W. and Winter, A.: Assemblages of coccolithophorids and other living microplankton off the coast
720 of Puerto Rico during January–May 1995, Mar. Micropaleontol., 39(1–4), 113–130, doi:10.1016/S0377-
721 8398(00)00017-7, 2000.

Kaffes, A.: Carbon and nitrogen fluxes in the marine coccolithophore Emiliania huxleyi grown under different nitrate concentrations, J. Exp. Mar. Biol. Ecol., 393, 1–8, doi:10.1016/j.jembe.2010.06.004, 2010.

Keller, M., Selvin, R., Claus, W. and Guillard, R.: Media for the culture of oceanic ultraphytoplankton, J. Phycol., 23, 633–638, 1987.

Klaas, C. and Archer, D. E.: Association of sinking organic matter with various types of mineral ballast in the deep sea: Implications for the rain ratio, Glob. Biogeochem. Cycles, 16(4), 1116, doi:10.1029/2001GB001765, 2002.

Klausmeier, C. A. and Litchman, E.: Algal games: The vertical distribution of phytoplankton in poorly mixed water columns, Limnol Ocean., 46(8), 1998–2007, 2001.

Krug, S. A., Schulz, K. G. and Riebesell, U.: Effects of changes in carbonate chemistry speciation on Coccolithus braarudii: a discussion of coccolithophorid sensitivities, Biogeosciences, 8(3), 771–777, doi:10.5194/bg-8-771-2011, 2011.

Labry, C., Youenou, A., Delmas, D. and Michelon, P.: Addressing the measurement of particulate organic and inorganic phosphorus in estuarine and coastal waters, Cont. Shelf Res., 60, 28–37, doi:10.1016/j.csr.2013.04.019, 2013.

Langer, G., Geisen, M., Baumann, K.-H., Kläs, J., Riebesell, U., Thoms, S. and Young, J. R.: Species-specific responses of calcifying algae to changing seawater carbonate chemistry, Geochem. Geophys. Geosystems, 7(9), 155–161, doi:10.1029/2005GC001227, 2006.

Langer, G., Gussone, N., Nehrke, G., Riebesell, U., Eisenhauer, A. and Thoms, S.: Calcium isotope fractionation during coccolith formation in Emiliania huxleyi: Independence of growth and calcification rate, Geochem. Geophys. Geosystems, 8(5), Q05007, doi:10.1029/2006GC001422, 2007.

Langer, G., Oetjen, K. and Brenneis, T.: Calcification of Calcidiscus leptoporus under nitrogen and phosphorus limitation, J. Exp. Mar. Biol. Ecol., 413, 131–137, doi:10.1016/j.jembe.2011.11.028, 2012.

Langer, G., Oetjen, K. and Brenneis, T.: Coccolithophores do not increase particulate carbon production under nutrient limitation: A case study using Emiliania huxleyi (PML B92/11), J. Exp. Mar. Biol. Ecol., 443, 155–161, doi:10.1016/j.jembe.2013.02.040, 2013.

LaRoche, J., Rost, B. and Engel, A.: Bioassays, batch culture and chemostat experimentation, Riebesell, U., Fabry, V.J., Hansson, L., Gattuso, J.-P. (Eds.), Guide to Best Practices for Ocean Acidification Research and Data Reporting. Publications Office of the European Union., 2010.

Laws, E. A.: Evaluation of In Situ Phytoplankton Growth Rates: A Synthesis of Data from Varied Approaches, Annu. Rev. Mar. Sci., 5(1), 247–268, doi:10.1146/annurev-marine-121211-172258, 2013.

Leonardos, N. and Geider, R. J.: Elevated atmospheric carbon dioxide increases organic carbon fixation by Emiliania huhleyi (Haptophyta), under nutrient-limited high-light conditions., J. Phycol., 41(6), 1196–1203, doi:10.1111/j.1529-8817.2005.00152.x, 2005.

Litchman, E., Klausmeier, C. A., Schofield, O. M. and Falkowski, P. G.: The role of functional traits and trade-offs in structuring phytoplankton communities: scaling from cellular to ecosystem level, Ecol. Lett., 10(12), 1170–1181, doi:10.1111/j.1461-0248.2007.01117.x, 2007.

Loisel, H., Nicolas, J.-M., Sciandra, A., Stramski, D. and Poteau, A.: Spectral dependency of optical backscattering by marine particles from satellite remote sensing of the global ocean, J. Geophys. Res., 111(C09024), doi:10.1029/2005JC003367, 2006.

762 Lomas, M. W. and Glibert, P. M.: Comparisons of Nitrate Uptake, Storage, and Reduction in Marine Diatoms
763 and Flagellates, J. Phycol., 36(5), 903–913, doi:10.1046/j.1529-8817.2000.99029.x, 2000.

764 MacIntyre, H. L., Kana, T. M., Anning, T. and Geider, R. J.: Photoacclimation of Photosynthesis Irradiance
765 Response Curves and Photosynthetic Pigments in Microalgae and Cyanobacteria1, J. Phycol., 38(1), 17–38,
766 doi:10.1046/j.1529-8817.2002.00094.x, 2002.

767 Marañón, E., Cermeño, P., López-Sandoval, D. C., Rodríguez-Ramos, T., Sobrino, C., Huete-Ortega, M.,
768 Blanco, J. M. and Rodríguez, J.: Unimodal size scaling of phytoplankton growth and the size dependence of
769 nutrient uptake and use, Ecol. Lett., 16(3), 371–379, doi:10.1111/ele.12052, 2013.

770 Monod, J.: The Growth of Bacterial Cultures., Annual Review of Microbiology., 1949.

771 Morel, A., Gentili, B., Claustre, H., Babin, M., Bricaud, A., Ras, J. and Tièche, F.: Optical properties of the
772 "clearest" natural waters, Limnol. Oceanogr., 52(1), 217–229, doi:10.4319/lo.2007.52.1.0217, 2007.

773 Moutin, T., Karl, D. M., Duhamel, S., Rimmelin, P., Raimbault, P., Van Mooy, B. A. S. and Claustre, H.:
774 Phosphate availability and the ultimate control of new nitrogen input by nitrogen fixation in the tropical
775 Pacific Ocean, Biogeosciences, 5(1), 95–109, doi:10.5194/bg-5-95-2008, 2008.

776 Müller, M. N., Antia, A. N. and LaRoche, J.: Influence of cell cycle phase on calcification in the
777 coccolithophore Emiliania huxleyi, Limnol. Oceanogr., 53(2), 506–512, doi:10.4319/lo.2008.53.2.0506,
778 2008.

779 Müller, M. N., Beaufort, L., Bernard, O., Pedrotti, M. L., Talec, A. and Sciandra, A.: Influence of CO2 and
780 nitrogen limitation on the coccolith volume of Emiliania huxleyi (Haptophyta), Biogeosciences, 9(10), 4155–
781 4167, doi:10.5194/bg-9-4155-2012, 2012.

782 Okada, H. and McIntyre, A.: Seasonal distribution of modern coccolithophores in the western North Atlantic
783 Ocean, Mar. Biol., 54(4), 319–328, doi:10.1007/BF00395438, 1979.

784 Oviedo, A. M., Langer, G. and Ziveri, P.: Effect of phosphorus limitation on coccolith morphology and
785 element ratios in Mediterranean strains of the coccolithophore Emiliania huxleyi, J. Exp. Mar. Biol. Ecol.,
786 459, 105–113, 2014.

787 Paasche, E.: Reduced coccolith calcite production under light-limited growth: a comparative study of three
788 clones of Emiliania huxleyi (Prymnesiophyceae), Phycologia, 38(6), 508–516, doi:10.2216/i0031-8884-38-6-
789 508.1, 1999.

790 Paasche, E.: A review of the coccolithophorid Emiliania huxleyi (Prymnesiophyceae), with particular
791 reference to growth, coccolith formation, and calcification-photosynthesis interactions, Phycologia, 40(6),
792 503–529, doi:10.2216/i0031-8884-40-6-503.1, 2002.

793 Raimbault, P. and Garcia, N.: Evidence for efficient regenerated production and dinitrogen fixation in
794 nitrogen-deficient waters of the South Pacific Ocean: impact on new and export production estimates,
795 Biogeosciences, 5, 323–338, doi:10.5194/bg-5-323-2008, 2008.

796 Raimbault, P., Garcia, N. and Cerutti, F.: Distribution of inorganic and organic nutrients in the South Pacific
797 Ocean-evidence for long-term accumulation of organic matter in nitrogen-depleted waters, Biogeosciences,
798 5(2), 281–298, 2008.

799 Raven, J. A. and Crawfurd, K.: Environmental controls on coccolithophore calcification, Mar Ecol Prog Ser,
800 470, 137–166, doi:10.3354/meps09993, 2012.

801 Redfield, A. C.: The influence of organisms on the composition of sea-water, The Sea, 26–77, 1963.

802 Riegman, R., Stolte, W., Noordeloos, A. A. M. and Slezak, D.: Nutrient uptake and alkaline phosphatase (ec
803 3:1:3:1) activity of Emiliania huxleyi (PRYMNESIOPHYCEAE) during growth under N and P limitation in
804 continuous cultures, J. Phycol., 36(1), 87–96, doi:10.1046/j.1529-8817.2000.99023.x, 2000.

805 Rokitta, S. D. and Rost, B.: Effects of CO2 and their modulation by light in the life-cycle stages of the
806 coccolithophore Emiliania huxleyi, Limnol. Oceanogr., 57(2), 607–618, 2012.

807 Rost, B., Zondervan, I. and Riebesell, U.: Light-dependent carbon isotope fractionation in the
808 coccolithophorid Emiliania huxleyi, 2002.

809 Roth, P. H.: Distribution of coccoliths in oceanic sediments, in Coccolithophores, pp. 199–218, Cambridge.,
810 1994.

811 Rouco, M., Branson, O., Lebrato, M. and Iglesias-Rodríguez, M. D.: The effect of nitrate and phosphate
812 availability on Emiliania huxleyi (NZEH) physiology under different CO2 scenarios, Front. Aquat. Microbiol.,
813 4, 155, doi:10.3389/fmicb.2013.00155, 2013.

814 Sciandra, A., Harlay, J., Lefèvre, D., Leme, R., Rimmelin, P., Denis, M. and Gattuso, J.: Response of
815 coccolithophorid Emiliania huxleyi to elevated partial pressure of CO2 under nitrogen limitation, Mar. Ecol.
816 Prog. Ser., 261, 111–122, doi:10.3354/meps261111, 2003.

817 Selph, K. E., Landry, M. R., Taylor, A. G., Yang, E.-J., Measures, C. I., Yang, J., Stukel, M. R., Christensen, S.
818 and Bidigare, R. R.: Spatially-resolved taxon-specific phytoplankton production and grazing dynamics in
819 relation to iron distributions in the Equatorial Pacific between 110 and 140°W, Deep Sea Res. Part II Top.
820 Stud. Oceanogr., 58(3–4), 358–377, doi:10.1016/j.dsr2.2010.08.014, 2011.

821 Shutler, J. D., Land, P. E., Brown, C. W., Findlay, H. S., Donlon, C. J., Medland, M., Snooke, R. and Blackford,
822 J. C.: Coccolithophore surface distributions in the North Atlantic and their modulation of the air-sea flux of
823 CO2 from 10 years of satellite Earth observation data, Biogeosciences, 10(4), 2699–2709, doi:10.5194/bg-
824 10-2699-2013, 2013.

825 Terry, K. L.: Nitrate and phosphate uptake interactions in a marine Prymnesiophyte, J. Phycol., 18(1), 79–86,
826 doi:10.1111/j.1529-8817.1982.tb03159.x, 1982.

827 Trimborn, S., Langer, G. and Rost, B.: Effect of varying calcium concentrations and light intensities on
828 calcification and photosynthesis in Emiliania huxleyi, Limnol. Oceanogr., 52(5), 2285–2293,
829 doi:10.4319/lo.2007.52.5.2285, 2007.

830 Westbroek, P., Brown, C. W., Bleijswijk, J. van, Brownlee, C., Brummer, G. J., Conte, M., Egge, J., Fernández,
831 E., Jordan, R., Knappertsbusch, M., Stefels, J., Veldhuis, M., van der Wal, P. and Young, J.: A model system
832 approach to biological climate forcing. The example of Emiliania huxleyi, Glob. Planet. Change, 8(1–2), 27–
833 46, doi:10.1016/0921-8181(93)90061-R, 1993.

834 Winter, A., Henderiks, J., Beaufort, L., Rickaby, R. E. M. and Brown, C. W.: Poleward expansion of the
835 coccolithophore Emiliania huxleyi, J. Plankton Res., 36(2), 316–325, doi:10.1093/plankt/fbt110, 2014.

836 Young, J. R., Poulton, A. J. and Tyrrell, T.: Morphology of Emiliania huxleyi coccoliths on the northwestern
837 European shelf–is there an influence of carbonate chemistry?, Biogeosciences, 11(17), 4771–4782,
838 doi:10.5194/bg-11-4771-2014, 2014.

839 Zondervan, I.: The effects of light, macronutrients, trace metals and CO2 on the production of calcium
840 carbonate and organic carbon in coccolithophores—A review, Deep Sea Res. Part II Top. Stud. Oceanogr.,
841 54(5–7), 521–537, doi:10.1016/j.dsr2.2006.12.004, 2007.

842

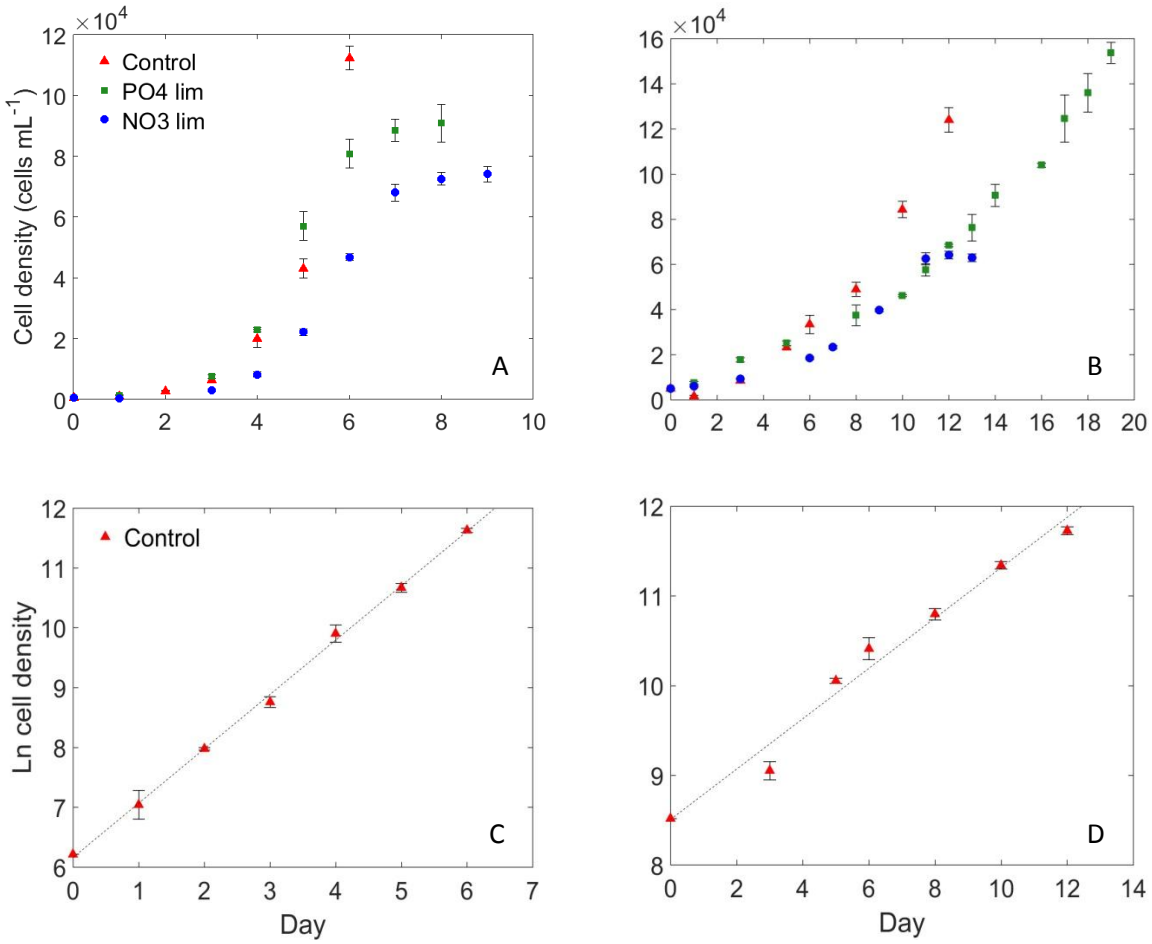

Figure 1. The evolution of cell density with time in culture experiments with *E. huxleyi* strain RCC911 (A: high irradiance; B: low irradiance) and cell density on a logarithmic scale for nutrient-replete cultures (C: high irradiance; D: low irradiance).

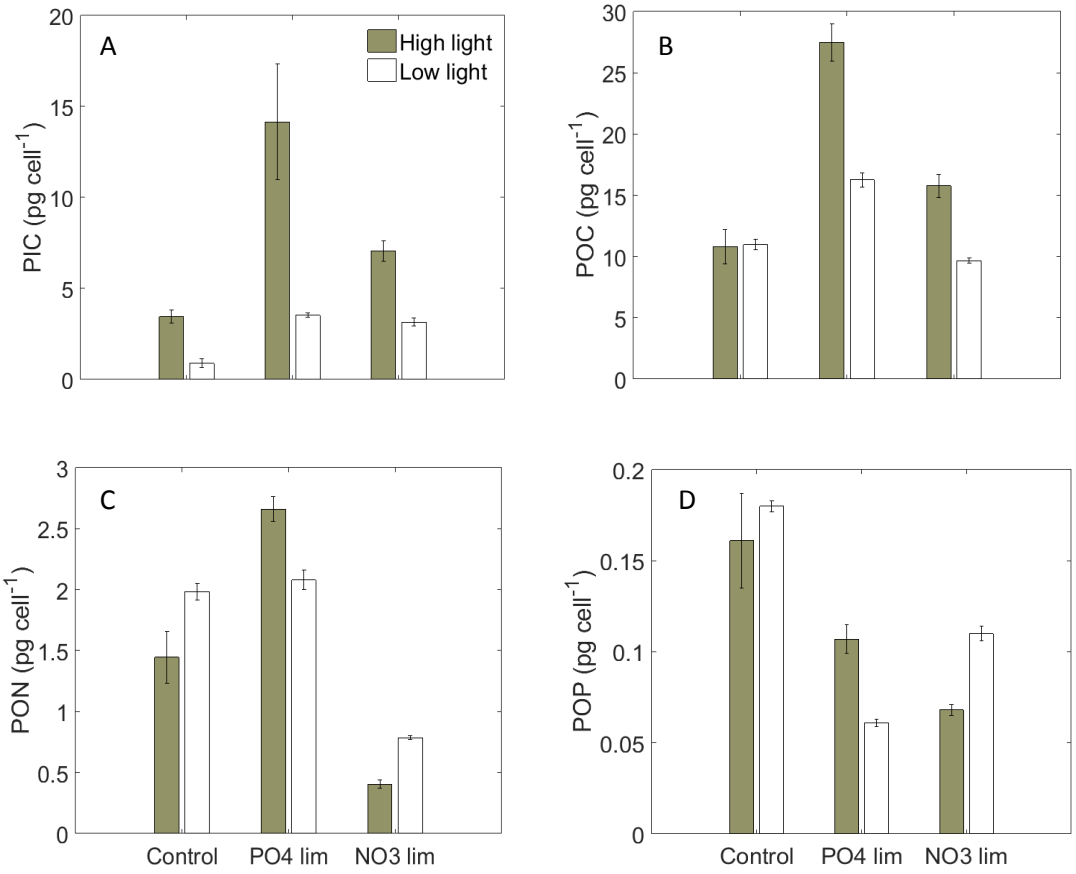

Figure 2. Cellular PIC (A), POC (B), PON (C), POP (D) quotas.

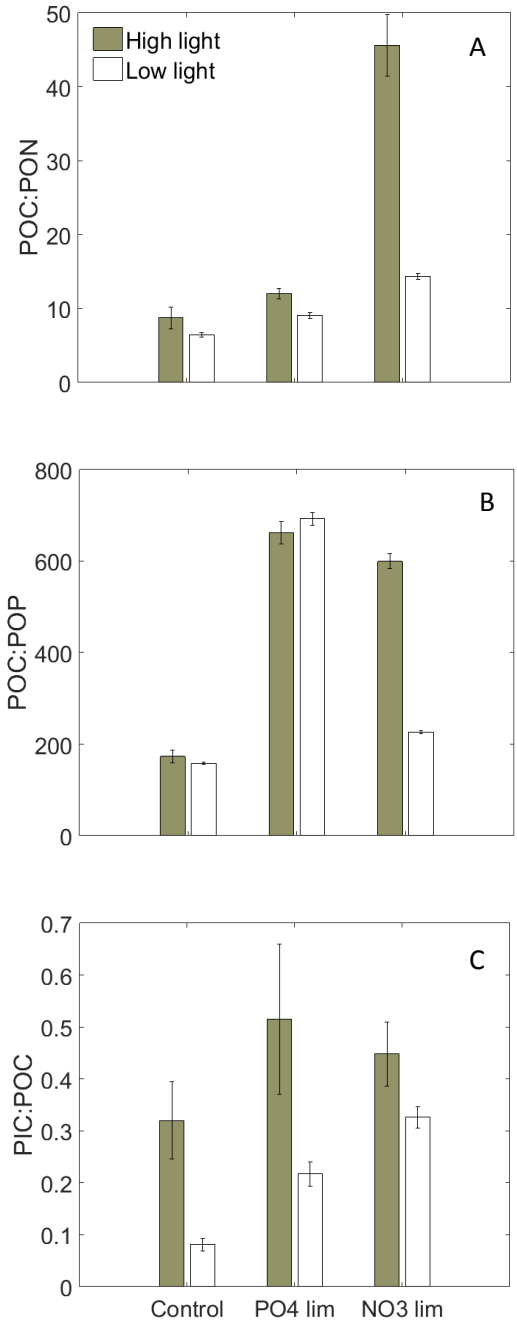

877

878

879

880 *Figure 3.* Cellular POC:PON (A), POC:POP (B) and PIC:POC (C) ratios.

881

882

883

884

885

886

887

888

889

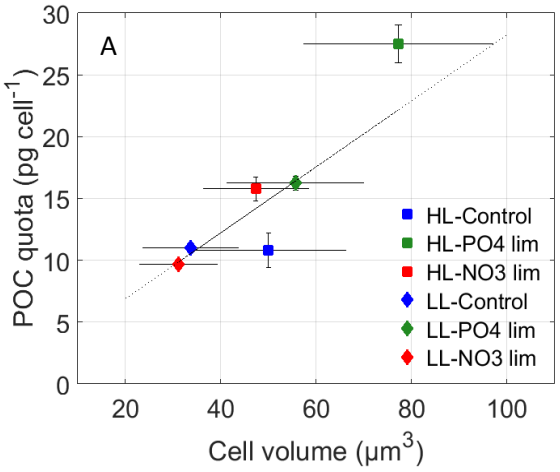

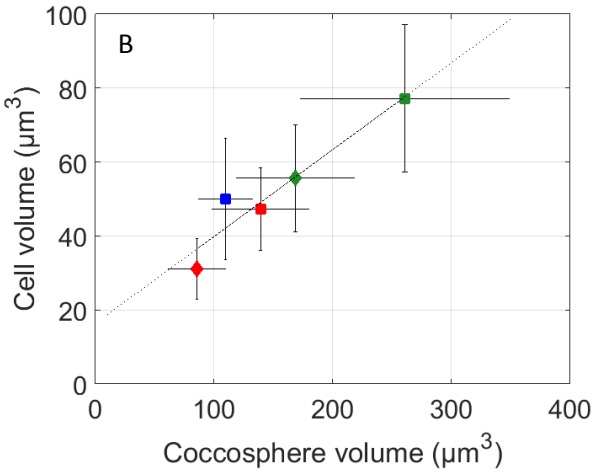

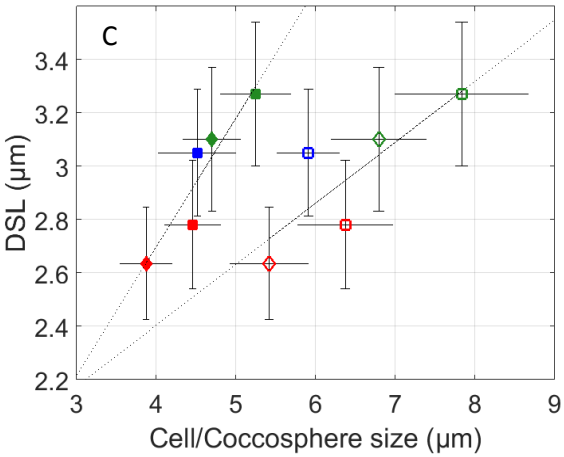

Figure 4. (A) POC quota versus cell volume; (B) Cell volume against coccosphere volume in high light (HL) and low light (LL) conditions; (C) Distal shield length (DSL) versus coccosphere and cell diameter. Solid symbols are cell size and open symbols are coccosphere size. Dotted line is the linear regression.

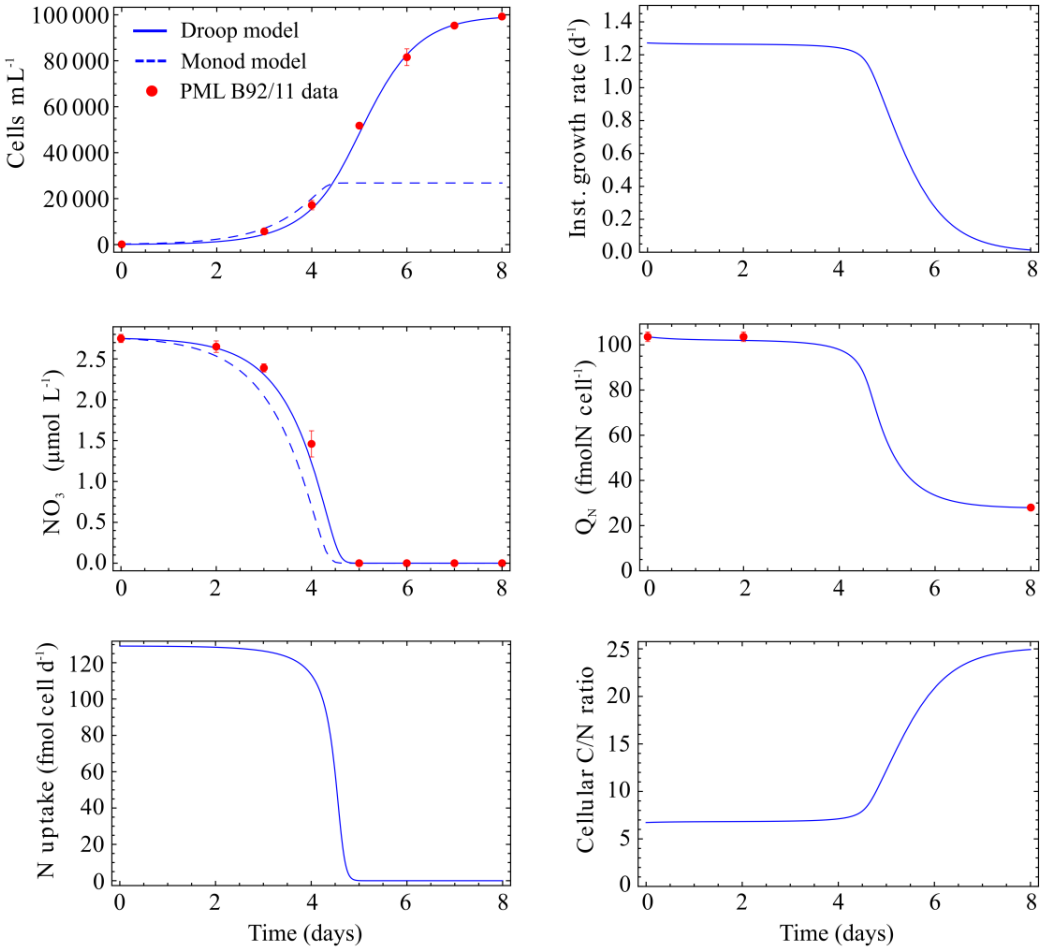

900

901 *Figure 5. Model fitted to the data of the nitrate-limited cultures of Langer et al. (2013) (Inst =*

902 *instantaneous).*

903

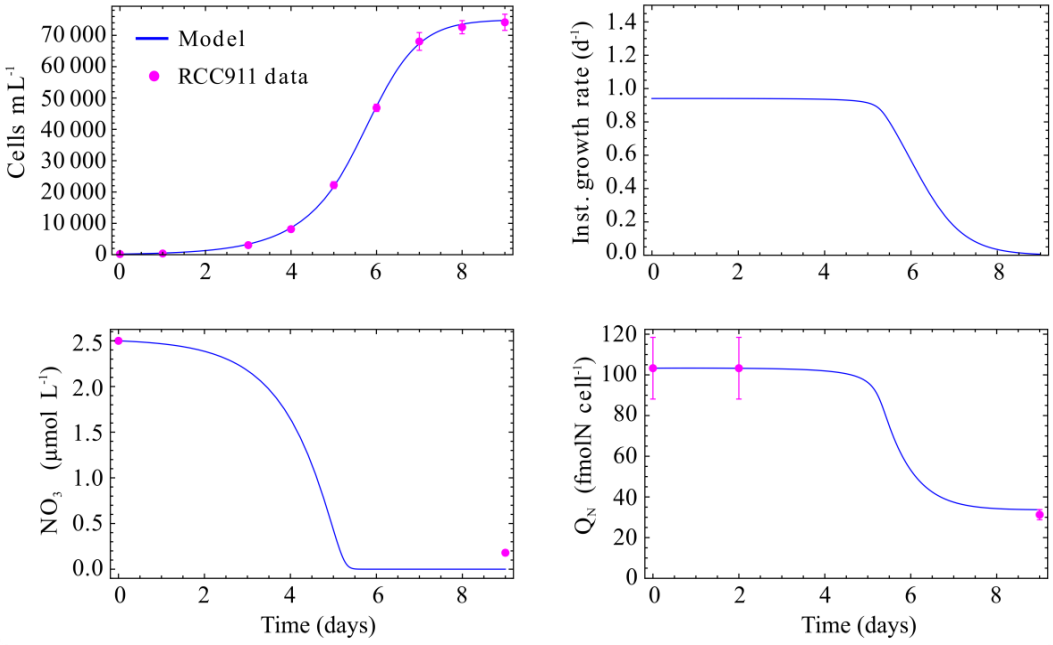

904

905 *Figure 6.* Model fitted to the data of the nitrate-limited cultures of strain RCC911 in high light conditions.

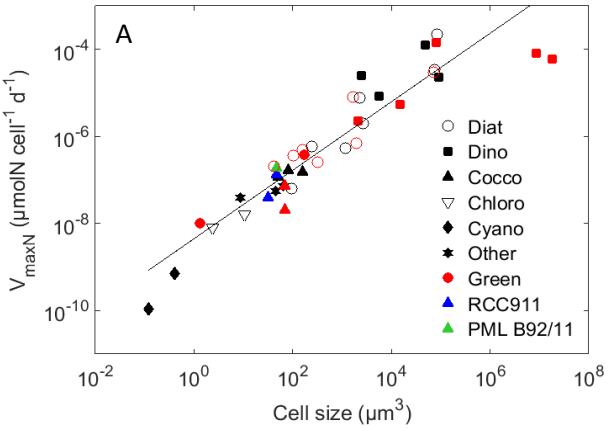

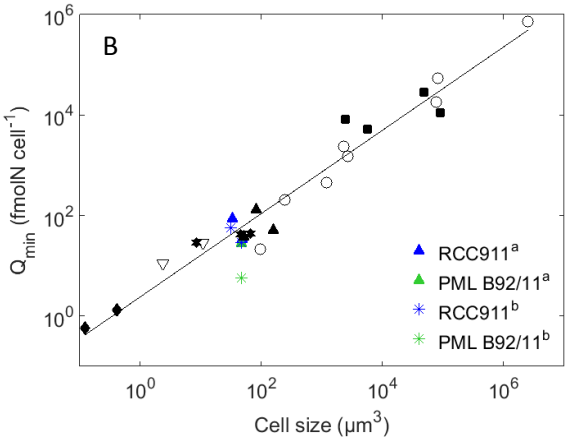

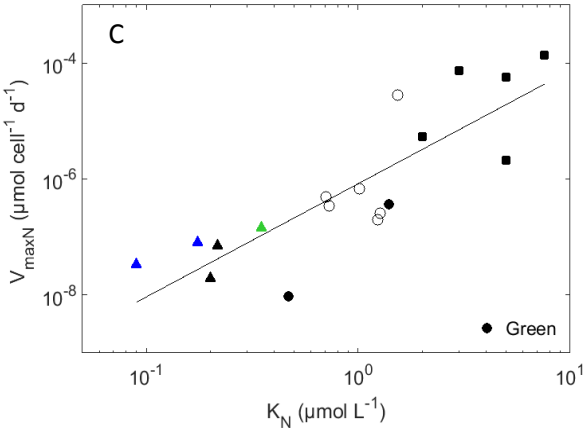

^{a} = model results; ^{b} = analysis results

Figure 7. A) Maximum normalized surface uptake rate V_{maxN} for nitrate versus the cell volume. Data from Marañón et al. (2013) in black, data from Litchman et al. (2007) in red and the Droop model output for the experiments presented in this work in blue and green depending of the strain; B) Minimum cellular quota Q_{min} for nitrate versus the cell volume. Data of Marañón et al. (2013) and the results from the model and analysis of the present study; C) V_{maxN} versus the half-saturation constant for nitrate uptake K_N. Data of Litchman et al. (2007) and results from the Droop model in nitrate-limited conditions.

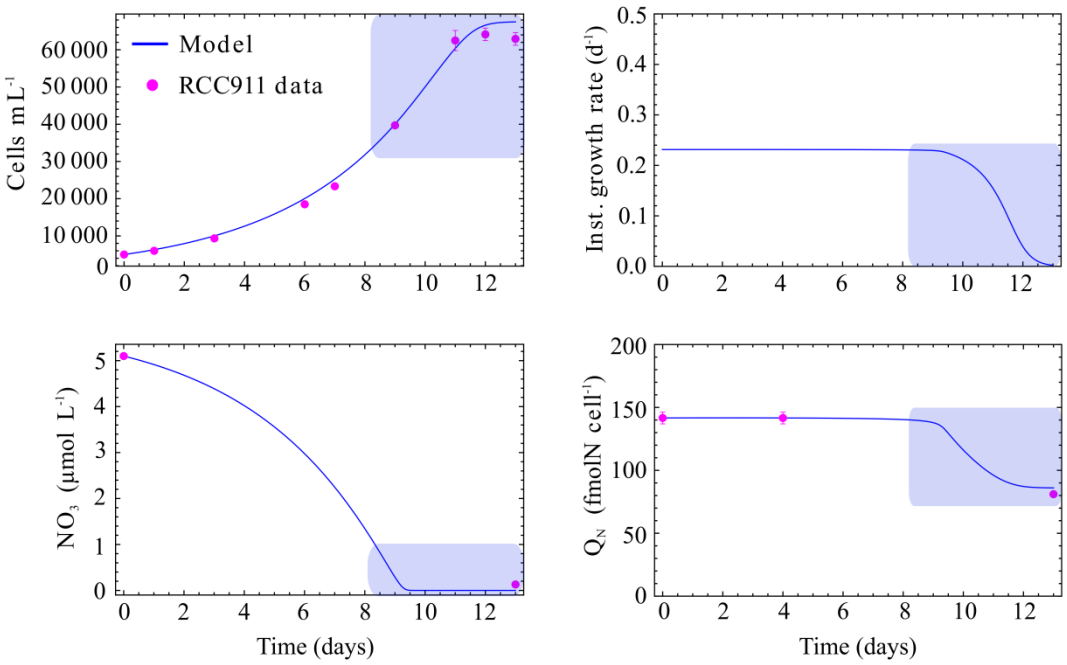

Figure 8. Model fitted to the data of the nitrate limited cultures on RCC911 strain in low light. The shaded area corresponds to the equivalent nitrate concentration in the BIOSOPE ecological niche of coccolithophores at the GYR station (between 150 and 200 m depth).

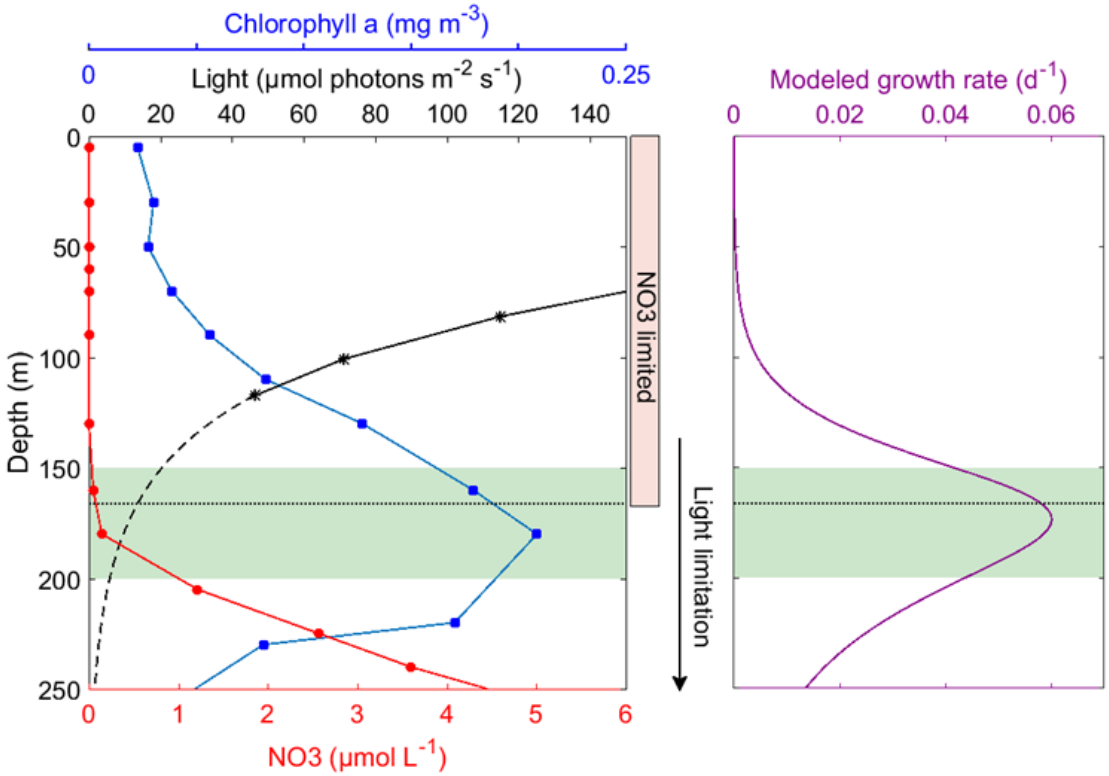

Figure 9. Left panel: In situ data (0 to 250 m) at the GYR station of the BIOSOPE transect (114.01° W, 26.06° S). Profiles of in situ measured chlorophyll a, PAR irradiance and nitrate concentration are shown. The dashed line represents an extrapolation of the irradiance between 117 m (last point measured) and 250 m considering a constant attenuation coefficient K_d (K_d=0.025 m^{-1} from Claustre et al., 2008) and a simple light calculation taken from MacIntyre et al. (2002). The dotted black line is the depth at which the K_N (0.09 µM) is observed. This depth also corresponds to the lower limit of nitrate limitation. Light limitation starts above the DCM and intensifies with depth. The green shaded area corresponds to the location of the maximum of coccosphere abundance taken from (Beaufort et al., 2008) between 120° W and 107° W. The right panel shows the growth rate of *E. huxleyi* with depth at the GYR station (calculated using Eq. A8).

Table 1. Growth rate, nutrient concentration, pH, DIC at the end of the experiments and shift in DIC compared with the initial DIC (averages from triplicate, n=3 for growth rates and nutrients analysis).

Sample	Growth rate[a]		NO3		PO4		pH		DIC		DIC shift
	d^{-1}	std	µmol L^{-1}	std	µmol L^{-1}	Std		std	µmol kg^{-1}	std	%
High light											
Control	0.91	*0.03*	67.92	*1.98*	3.95	*0.12*	8.13	*0.01*	2177	*19.14*	2.1
PO_4 lim	0.00		80.88	*0.35*	0.01	*0.00*	8.21	*0.01*	1894	*21.01*	12.1
NO_3 lim	0.00		0.18	*0.03*	5.74	*0.00*	8.14	*0.00*	2060	*3.61*	4.7
Low light											
Control	0.28	*0.01*	79.10	*1.15*	4.90	*0.04*	8.13	*0.02*	2161	*7.55*	4.1
PO_4 lim	0.13	*0.01*	75.25	*1.24*	0.01	*0.01*	8.30	*0.01*	1956	*8.33*	13.2
NO_3 lim	0.00		0.13	*0.02*	5.83	*0.02*	8.09	*0.00*	2139	*4.16*	39

[a] = cells are in exponential growth phase at the end of control experiments

Table 2. Cellular carbon, nitrogen and phosphorus quotas (averages from triplicate; n=6 for cellular quotas measurements).

Sample	PIC		POC		PON		POP		PIC:POC		POC:PON		POC:POP	
	pg $cell^{-1}$	std	pg $cell^{-1}$	std	pg $cell^{-1}$	std	pg $cell^{-1}$	std		std		std		std
High light														
Control	3.46	*0.36*	10.8	*1.38*	1.45	*0.21*	0.16	*0.03*	0.32	*0.05*	8.72	*1.45*	173	*14.0*
PO_4 lim	14.16	*3.19*	27.49	*1.53*	2.66	*0.10*	0.11	*0.01*	0.52	*0.12*	12.05	*0.70*	661	*24.3*
NO_3 lim	7.06	*0.55*	15.77	*0.95*	0.4	*0.04*	0.07	*0.00*	0.45	*0.04*	45.59	*4.12*	600	*16.7*
Low light														
Control	0.89	*0.10*	10.98	*0.41*	1.98	*0.07*	0.18	*0.00*	0.08	*0.01*	6.46	*0.28*	158	*2.51*
PO_4 lim	3.53	*0.25*	16.25	*0.56*	2.08	*0.08*	0.06	*0.00*	0.22	*0.017*	9.11	*0.41*	693	*13.4*
NO_3 lim	3.15	*0.13*	9.67	*0.21*	0.79	*0.02*	0.11	*0.00*	0.33	*0.015*	14.35	*0.37*	226	*3.38*

Table 3. Value of Q_R^{min} (which corresponds to the cellular PON (POP) at the end of the experiment: values measured and calculated) and the parameters obtained with the best-fit indicated for N and P limited experiment (high light: HL and low light: LL).

Strain	Light	Limitation	Q_R^{min}		Best-fit			
			Analysis	Calculation	V_{maxR}	K_R	μ_{max}	KQ_R
			fmol $cell^{-1}$	fmol $cell^{-1}$	µmol $cell^{-1}$ d^{-1}	µmol L^{-1}	d^{-1}	
PML B92/11		**NO_3**	5.71	27.7	$1.46.10^{-7}$	0.35	1.3	0.39
PML B92/11		**PO_4**	0.645	2.04	$1.36.10^{-8}$	0.051	1.57	0.98
RCC911	**HL**	**NO_3**	28.57	31.28	$1.05.10^{-7}$	0.205	1.01	0.25
RCC911	**HL**	**PO_4**	3.464	5.931	$1.47.10^{-8}$	0.35	1.2	0.9
RCC911	**LL**	**NO_3**	56.14	78.99	$3.34.10^{-8}$	0.09	0.2	0.3
RCC911	**LL**	**PO_4**	1.968	2.875	$5.74.10^{-10}$	0.275	0.52	0.47

963